nagra National Cooperative for the Disposal of Radioactive Waste

TECHNICAL REPORT 92-13

Characterisation of PWR Cladding Hulls from Commercial Reprocessing

December 1992

R. Restani, E.T. Aerne, G. Bart,
H.P. Linder, A. Müller, F. Petrik

PSI, Würenlingen and Villigen

Hardstrasse 73, CH-5430 Wettingen / Switzerland, Telephone +41-56-37 11 11

nagra National Cooperative for the Disposal of Radioactive Waste

TECHNICAL REPORT 92-13

Characterisation of PWR Cladding Hulls from Commercial Reprocessing

December 1992

R. Restani, E.T. Aerne, G. Bart,
H.P. Linder, A. Müller, F. Petrik

PSI, Würenlingen and Villigen

Hardstrasse 73, CH-5430 Wettingen / Switzerland, Telephone +41-56-37 11 11

This report was prepared as an account of work sponsored by Nagra. The viewpoints presented and conclusions reached are those of the author(s) and do not necessarily represent those of Nagra.

FOREWORD

The Swiss nuclear power plant companies have signed reprocessing contracts with COGEMA and BNFL for their spent fuel. Hulls and ends will be conditioned in cement and can be returned to Switzerland as waste to be disposed of by NAGRA. With a view to developing characterisation techniques, NAGRA agreed with the CEA under an existing information exchange agreement to participate in the CEA characterisation work on hulls reprocessed by COGEMA on an industrial scale. The work was carried out by PSI. The results were published by the CEA in an EUR report in 1986 and by PSI in a technical communication (in German) in 1991. This report is essentially an English translation of the PSI paper intended for a wider external distribution and as a complement to the CEA report. We note that the Swiss results are quoted in the COGEMA specification of hulls and ends issued in March 1990.

ABSTRACT

Hull and structure material debris from a fuel element of the PWR Obrigheim reprocessed on an industrial scale have been investigated with main emphasis on determining nuclide-specific activity concentrations resulting from fuel element irradiation and contamination during the chop-leach process.

Different methods were used to measure the actinide concentrations and their isotopic compositions. In the case of fission and activation products, investigations were restricted to nuclides which were measurable using gamma spectrometry.

Additional studies, which contributed to understanding cladding contamination and assessing the Zircaloy material and its surface, were performed using SIMS depth profile analysis, α-autoradiography and microscopic investigations.

SUMMARY

Within the framework of the EC characterisation programme COQUENSTOCK and the cooperation agreement between NAGRA and the CEA, PSI received 2 kg of leached hull residues (hull and structure material debris) from the UP2-400 reprocessing plant in La Hague for radiochemical investigation.

The contaminated and activated hull material originated from a fuel element of the PWR Obrigheim (Germany), which had an average burn-up of 30 GWd/tU. The spent fuel from the chopped fuel element was dissolved in a static dissolver and then rinsed.

Because of the significance for repository safety analyses, the emphasis of the investigations was placed on measuring the α-isotope composition, the actinide concentrations and the local distribution of these on and in the fuel element hulls.

The main activity in the cladding waste can be attributed to the presence of typical activation products in the fuel element structural materials, which consist of Inconel and stainless steel. After a cooling period of five years, the gamma dose rate from these components is generally more than a factor of 30 higher than that from the Zircaloy-4 fuel rod fragments (Table a). The Co-60 activities vary very widely and reflect the differing content of Co-59 in the non-irradiated structural material. In the case of the Zircaloy hulls, the activity is dominated by Sb-125 from the Zircaloy alloying element tin, and by fission products (Table b). The fission products significantly contaminate the structure material in the dissolver.

The isotope dilution analysis following chemical dissolution of the Zircaloy hulls gave uranium concentrations of 400 to 2,150 mg U/kg Zry, with a mean value of 1,130 ppm. The Pu/U weight ratio of 1:85 is found to be relatively constant over the whole contamination range. It is also worth noting that the U- and Pu-isotopic composition remains constant in spite of local differences in burn-up (form factor = 1.15). In addition, the Pu-isotopic composition on the Zircaloy hulls is not found to reflect the values which are expected for undissolved, adherent fuel, so that deposition processes during the fuel dissolution can be taken as determining the α-contamination of the hulls.

Based on α-spectrometry measurements, it can be stated that, besides the Pu isotopes, the nuclides Am-241 and Cm-244 contribute more than 30 % to the mean total α-activity of 6.7 mCi/kg Zry (= 250 MBq/kg Zry) (Table b).

The activity distribution on and in the Zircaloy hulls was investigated using α-autoradiography and secondary ion mass spectrometry (SIMS). The Zircaloy surfaces are completely contaminated both inside and outside. Due to the dissolution and flushing processes, the outside surface has a relatively even α-contamination while, on the inside surface (in contact with the fuel) localised areas with very high contamination occur frequently. These areas are formed by

residues of dried fuel solution and are particularly significant for trapped residues in pinched or deformed hulls. These localised areas are characterised by the loosely bound nature of the α-deposits.

Qualitative SIMS depth profile analysis showed that uranium is deposited or emplaced almost exclusively on the surface and, to a small extent, in the thin oxide layer. Compared to this, the fission products penetrate further into the inner surface due to their recoil energy. This implanted beta,gamma activity is significant and very difficult to remove by rinsing. On the other hand, the primary α-contamination on the inner surface was largely removed by the very efficient fuel dissolution process. The secondary contamination on the hulls, especially on the inner surface, arising in the dissolver could be washed out to a greater extent by using a more suitable rinsing procedure which takes into account hull deformation and the somewhat rough surface structure. On the outside of the hulls, the concentrations tend to be regular and fit the concept of a purely secondary surface contamination.

Since the contamination mechanism for the fission products is different to a certain extent from that for the actinides, it is understandable that the correlation between the actinides and the fission products is limited. When characterising the cladding waste, Cs-137 is therefore not really suitable as a reference nuclide for the adhesive, fissile material.

Table a: Dose rate and β–, γ-activities of cladding debris (110 pieces, 0.528 kg) from the UP-2 reprocessing of a spent fuel element 5 years after discharge from PWR Obrigheim (Burn-up: 30 GWd/tU)

Material	γ-Dose rate at 50 cm and Standard Deviation per sample [mR/h]	Typical Fission Product Activity and Standard Deviation [mCi/kg waste]		Typical Activation Product Activity and Standard Deviation [mCi/kg waste]	
		Cs-137	Ru-106	Co-60	Mn-54
ZIRCALOY-4 (Hulls)	25 ± 8	540 ± 29 %	460 ± 36 %	64 ± 30 %	3.4 ± 16 %
STAINLESS STEEL INCONEL (Structure material)	900 ± 750	~ 300 ± 85 %	370	18'500 ± 55 %	325 ± 100 %
CLADDING DEBRIS (73 wt-% Zircaloy-4, 27 wt-% S.S. + Inconel)	(~ 200)	~ 480	~ 440	~ 5'000	~ 90

Table b: Summary of the α-, β-, γ-activities and actinide concentrations in Zircaloy hulls of a spent fuel element from PWR Obrigheim after reprocessing in UP-2 (5 years cooling time)

β-,γ-NUCLIDES	β-,γ-ACTIVITIES [mCi/kg Zry]
Mn- 54	3.4
Co- 60	64
Sr- 90	370
Ru-106	458
Sb-125	760
Cs-134	162
Cs-137	542
Ce-144	70
Eu-154	21
α-NUCLIDES	**α-ACTIVITIES [mCi/kg Zry]**
Pu-238	3.12 (1) } 4.6 (2)
Pu-239 + Pu-240	1.24 (1) }
Am-241	0.92 (2)
Cm-244	1.26 (2)
	6.7 (2)
ACTINIDES	**CONCENTRATIONS AND STANDARD DEVIATIONS [mg/kg Zry]**
URANIUM (98.4 % U-238, 1.19 % U-235, 0.38 % U-236, 0.025 % U-234) (3)	1132 ± 446 (1)
PLUTONIUM (61 % Pu-239, 23.1 % Pu-240, 10.1 % Pu-241, 4.46 % Pu-242, 1.33 % Pu-238) (3)	13.6 ± 5.0 (1)
NEPTUNIUM	0.35 ± 0.14

(1) Mass spectrometry
(2) α-spectrometry
(3) Weight %

RÉSUMÉ

Dans le cadre du programme de caractérisation "COQUENSTOCK" de la C.E. et de la collaboration CEA-Cédra, l'IPS a reçu 2 kg de débris de coques et pièces métalliques associées provenant de l'usine de retraitement UP2-400 à la Hague pour réaliser ses propres investigations radiochimiques.

Les matériaux contaminés et activés provenaient d'un élément de combustible du réacteur à eau sous pression d'Obrigheim (Allemagne) présentant un taux de combustion moyen de 30 GWd/tU. Le combustible de l'élément cisaillé avait été dissous dans un appareillage statique et rincé.

En raison de leur signification pour les analyses de sûreté d'un dépôt final, l'accent des travaux s'est porté sur la détermination des isotopes α et des concentrations d'actinides ainsi que de leur distribution spatiale à la surface extérieure et intérieure des gaines de combustible.

L'activité principale des déchets de gainages est due à la présence de produits d'activation typiques de l'inconel et de l'acier inoxydable utilisés pour les pièces de structure des éléments de combustible. Après une durée de refroidissement de 5 ans, la dose γ de ces pièces de structure est en moyenne de plus d'un facteur 30 comparée à celle des coques en zircaloy-4 (Table a, page IV). Les activités dues au Co-60 varient toutefois considérablement et reflètent les différences de teneur en Co-59 des matériaux de structure avant irradiation. En ce qui concerne les coques en zircaloy, c'est le Sb-125 issu de l'étain, un élément d'alliage du zircaloy, et les produits de fission qui dominent (Table b, page V). Ces derniers contaminent aussi de façon significative les éléments de structure dans le bain de dissolution.

Les analyses isotopiques, après dissolution chimique des gaines de zircaloy, ont livré des teneurs en uranium entre 400 et 2'150 mg U/kg Zry, la moyenne étant de 1'130 ppm. Pour toutes ces concentrations on trouve un rapport de poids Pu/U relativement constant de 1:85. Il faut en outre relever la constance de la composition isotopique de l'U et du Pu, malgré des taux de combustion axiaux légèrement variables (facteur de forme = 1.15). De plus, la composition isotopique du Pu sur le zircaloy indique une tendance que l'on n'attendrait guère d'un combustible adhérent non-dissout, ce qui conduit à considérer les processus de déposition durant la dissolution du combustible comme déterminants pour la contamination α des coques.

Les mesures de spectrométrie α ont montré qu'en sus des isotopes du Pu les radionucléides Am-241 et Cm-244 contribuent pour plus de 30 % à l'activité α globale moyenne de 6,7 mCi/kg Zry (= 250 MBq/kg Zry) (Table b, page V).

La distribution des activités à l'extérieur et à l'intérieur des gaines en zircaloy a été étudiée par autoradiographie α et spectrométrie de masse à ions secondaires (SIMS). Les surfaces de zircaloy sont contaminées sans lacunes, à l'intérieur comme à l'extérieur. La surface extérieure présente une contami-

nation relativement régulière résultant du processus de dissolution et de rinçage, alors que l'on relève souvent sur la face côté combustible des zones de très forte contamination. On remarque que ces dépôts α très concentrés, qui sont des résidus piégés et séchés, apparaissant particulièrement sur les coques fortement déformées, sont relativement peu adhérents.

Des analyses qualitatives par SIMS de profils en profondeur ont montré que l'uranium n'était pratiquement présent qu'en surface et, dans une très faible mesure seulement, dans la fine couche d'oxyde. Les produits de fission, par contre, pénètrent plus loin dans la face intérieure en raison de leur énergie de recul. Cette activité β et γ implantée non-négligeable ne peut guère être éliminée par rinçage. La contamination primaire alpha sur la surface intérieure a été largement éliminée par l'efficace procédé de dissolution du combustible. Un processus de rinçage plus approprié, tenant compte de la déformation des gaines et de la surface partiellement rugueuse, pourrait permettre aussi d'éliminer une bonne partie de la contamination secondaire produite dans le dissolveur. Sur la surface extérieure, la distribution des concentrations est presque homogène et correspond à ce que l'on peut attendre d'une contamination uniquement secondaire.

Le mécanisme de contamination des produits de fission étant différent en partie de celui des actinides, il est compréhensible qu'il n'existe qu'une très faible corrélation entre eux. Il en résulte que le Cs-137 se prête plutôt mal comme nucléide significatif pour la charactérisation de débris de coques en ce qui concerne les matériaux fissiles adhérents.

ZUSAMMENFASSUNG

Aus dem EG-Charakterisierungsprogramm COQUENSTOCK über Brennstabhülsen, erhielt das PSI, im Rahmen der Zusammenarbeit zwischen dem CEA und der NAGRA, 2 kg ausgelaugte Hülsenreststücke aus der Wiederaufarbeitungsanlage UP2-400 in La Hague zur eigenen radiochemischen Untersuchung.

Das kontaminierte und aktivierte Hülsenmaterial stammte von einem zerlegten Brennelement des PWR Obrigheim (BRD) mit einem mittleren Abbrand von 30 GWd/tU. Die Hülsen wurden in einem statisch arbeitenden Auflösebad behandelt und dann gespült.

Wegen der Bedeutung für die Endlager-Sicherheitsanalysen lag das Schwergewicht der Arbeiten auf der Bestimmung der α-Isotopenzusammensetzung, der Actinidenkonzentrationen und der örtlichen Verteilung derselben auf und in den Brennstabhülsen.

Die Hauptaktivität des Cladding-Abfalls ist auf die Anwesenheit typischer Aktivierungsprodukte in den aus Inconel und rostfreiem Stahl bestehenden BE-Strukturmaterialien zurückzuführen. Die γ-Dosisleistung dieser Strukturteile liegt nach 5 jähriger Abkühlzeit im Mittel um mehr als einen Faktor 30 höher als diejenige der Zircaloy-4-Brennstabstücke (Tabelle a, Seite IV). Die Co-60 Aktivitäten variieren dabei allerdings sehr stark und widerspiegeln den unterschiedlichen Gehalt an Co-59 im unbestrahlten Strukturmaterial. Demgegenüber dominieren bei den Zircaloy-Hülsen Sb-125 vom Zircaloy-Legierungselement Zinn, sowie die Spaltprodukte (Tabelle b, Seite V). Mit letzteren werden im Auflösebad auch die Strukturteile in erheblichem Masse kontaminiert.

Die Isotopenverdünnungsanalyse nach chemischer Auflösung von Zircaloy-Hülsen ergab Urankonzentrationen von 400 bis 2'150 mg U/kg Zry bei einem Mittelwert von 1'130 ppm. Über den gesamten Kontaminationsbereich besteht ein mässig konstantes Pu/U-Gewichtsverhältnis von 1:85. Bemerkenswert ist im weiteren die konstante U- und Pu-Isotopenzusammensetzung trotz axial leicht unterschiedlicher Abbrände (Formfaktor = 1.15). Zusätzlich weist die Pu-Isotopenzusammensetzung am Zircaloy in eine Richtung, wie man sie für anhaftenden, ungelösten Brennstoff kaum erwarten würde, so dass Ablagerungsvorgänge während der Brennstoffauflösung als entscheidend für die α-Kontamination der Brennstabhülsen gewertet werden.

Aufgrund α-spektrometrischer Messungen tragen neben den Pu-Isotopen die Nuklide Am-241 und Cm-244 mehr als 30 % zur mittleren α-Gesamtaktivität von 6,7 mCi/kg Zry (= 250 MBq/kg Zry) bei (Tabelle b, Seite V).

Die Aktivitätsverteilung auf und in den Zircaloy-Hülsen wurde mittels α-Autoradiographie und Sekundärionen-Massenspektroskopie (SIMS) untersucht. Die Zircaloyoberflächen sind lückenlos sowohl innen wie aussen kontaminiert. Die Aussenseite weist durch den Auflöse- und Spülprozess eine relativ gleichmäs-

sige α-Kontamination auf, während auf der Brennstoffseite häufig lokale Bereiche sehr hoher Kontamination auszumachen sind. Typisch für diese hochkonzentrierten Stellen, welche durch eingetrocknete Lösungsreste entstanden sind und bei stark deformierten Hülsen besonders ausgeprägt auftreten, ist die relativ lose Beschaffenheit dieser α-Rückstände.

Qualitative SIMS-Tiefenprofilanalysen zeigten, dass Uran fast ausschliesslich auf der Oberfläche und in geringem Ausmass in der dünnen Oxidschicht ab- bzw. eingelagert wird. Demgegenüber dringen die Spaltprodukte durch die Rückstossenergie ziemlich weit in die Innenoberfläche ein. Diese bedeutende, implantierte β, γ-Aktivität kann beim Spülen kaum entfernt werden. Hingegen liess sich die primäre α-Kontamination auf der Innenseite durch den effizienten Auflösungsprozess weitgehend entfernen. Die sekundäre Kontamination der Hülsen im Auflöser könnte ebenfalls in einem geeigneten Spülverfahren, welche der Hülsenverformung und der teilweise rauhen Oberflächenstruktur Rechnung trägt, zu einem grösseren Teil ausgewaschen werden. Auf der Aussenseite sind die Konzentrationsverläufe gleich und entsprechen der Vorstellung einer lediglich oberflächlich entstandenen sekundären Kontamination.

Da für die Spaltprodukte teilweise ein anderer Kontaminationsmechanismus als für die Actiniden verantwortlich zeichnet, ist es verständlich, dass zwischen ihnen eine nur sehr bescheidene Korrelation besteht. Bei der Charakterisierung des Cladding-Abfalls eignet sich deshalb Cs-137 eher schlecht als Leitnuklid für das anhaftende, spaltbare Material.

TABLE OF CONTENTS

1 INTRODUCTION

1.1 Overview

During reprocessing of spent fuel elements, the fuel rods are chopped into pieces a few cm in length and the spent fuel content is dissolved in an acid solution. The remaining hulls are contaminated with actinides and fission products. In addition to the Zircaloy hulls, there are other activated metallic components such as spacers, endcaps, springs, etc.

The characterisation of the hulls is of interest not only for the safety of waste disposal but also for improving the reprocessing process. Knowledge of the residual activities and of their fixation processes on the hulls (adhesive undissolved fuel, radionuclide implantation through decay recoil, contamination through radioelements dissolved in the acid solution) allows better modelling of radionuclide release in the disposal safety analysis and better elimination of these radionuclides during reprocessing through adapted fuel dissolution and hull rinsing. (As a result static dissolvers are now replaced by rotating dissolvers).

After vitrified residue (HLW), hulls and endcaps (ILW) represent one of the most radiologically hazardous reprocessing wastes. The hulls and ends conditioned in cement are classified by NAGRA as "LMA" waste ("langlebige mittelaktive Abfälle" or intermediate level waste with long-lived radionuclides), and will be disposed of in a "LMA" repository adjacent to the HLW repository.

1.2 Previous investigations

Initial radiochemical investigations of leached fuel element hulls had already been carried out by the CEA/FAR (GUÉ et al. 1982), UKAEA/Harwell (JENKINS et al. 1982), LASL (REILLY, T.D. 1979), BNWL/Battelle (DILLON, R.L. 1986), KfK/Karlsruhe (WERTENBACH, H. 1984) and other institutes. These works have been summarised and published as a monograph by the European Community (HEBEL & COTTONE 1982). The disadvantage of these early studies was that the fuel elements were generally processed under laboratory-type conditions and it was therefore impossible to draw any direct conclusions for the case of cladding debris from reprocessing on an industrial scale.

As a follow-up, the CEA, in collaboration with the EC, launched the COQUENSTOCK investigation programme with the aim of obtaining large quantities of hulls directly from the COGEMA reprocessing plant at La Hague and analysing the material in suitably equipped laboratories. Cladding debris from two different sources was investigated, both originating from the static HAO dissolver of the UP-2 facility. Coquenstock 1-hulls came from one fuel element of the PWR Obrigheim (Germany), while the Coquenstock 2-hulls came from 2 1/2 fuel elements of the PWR Stade (also Germany).

The analyses included overview studies, gamma spectrometry, passive neutron measurement (estimate of the Pu content), isotope dilution analysis, α-spectrometry, measurement of volatile fission products and hydrogen content as well as experiments on cleaning of the hulls.

The analyses and associated results have been published in the form of an EC report (GUÉ et al. 1987). This provides a comprehensive (radio)chemical description of cladding contamination and, with a view to industrial reprocessing, investigates the cleaning potential for reducing the contamination and checking the actinide content of the cladding waste by means of neutron measurement.

1.3 PSI work

Based on NAGRA's interest in hull characterisation for disposal purposes as well as on PSI's interest in nuclear chemistry within the framework of its development work for waste disposal, a joint approach was therefore made to the CEA (Commissariat à l'Energie Atomique, France) to clarify the extent to which PSI could participate in the "COQUENSTOCK" hull characterisation programme of the European Community. Within the overall framework of the existing CEA/NAGRA cooperation agreement, the CEA was willing to make available 2 l of active hull material from a pressurised water reactor for experimental purposes, the aim being to achieve as precise a characterisation as possible of the cladding hulls. Associated with this was the task of comparing the results of similar types of analyses and including supplementary analytical techniques (including SIMS depth profile studies) in the investigation.

Following discussions with interested parties, the cladding characterisation programme at PSI was structured as follows:

1. Overview analysis

- visual assessment of the hulls
- beta/gamma activity measurements using gamma spectrometry
- dose rate measurements
- measuring qualitative α-activity distribution at the hull surface using α-autoradiography
- determining fixed contamination after cleaning of Zircaloy hulls

2. Analysis following chemical dissolution of Zircaloy hulls

- isotope dilution analysis
  (mass spectrometric measurement of U-, Pu-isotopic composition)
- α-spectrometry
  (total α-activity, Am-241 and Cm-244 activity)
- neutron activation analysis of Np-237

3. Surface investigations

- SIMS depth profile analysis
  (penetration of the surface by uranium and fission products)
- light optical microscopy of polished cross-sections
  (oxide layer thicknesses)
- scanning electron microscopy
  (structure of the inner surface)

This summary report discusses the results of the cladding investigations carried out at PSI.

1.4 Closing remarks

The hulls investigated in this work are a subsample of the hulls investigated in the COQUENSTOCK work. They originate from the COGEMA UP-2/HAO facility which is equipped with a static dissolver. The Swiss spent fuel will be reprocessed in the new UP-3 plant built for the base load customers, which is equipped with a rotating dissolver. The present results are therefore not directly applicable to the hulls and ends to be disposed of in Switzerland as the fuel dissolution and the hull rinsing will be improved.

2 FUEL ELEMENT PROPERTIES AND REPROCESSING

The hull material, which was made available to PSI through NAGRA by the CEA, originates from Coquenstock 1 and therefore relates to a fuel element from the PWR Obrigheim (Germany).

The key data are as follows (GUÉ et al. 1987):

Fuel element type	: 14 x 14
Number of fuel rods	: 180
Length of fuel rods	: 2.9 m
Hull diameter	: 10.75 mm (outer)
Hull thickness	: 0.72 mm
Fuel rod material	: Zircaloy-4 (80 kg)
Structural material	: - Inconel 718 (6.2 kg) - stainless steel (9.7 kg) - aluminium oxide (1 kg)
Original enrichment	: 3.21 % U-235 from 276 kg U
Burn-up	: 30 GWd/tU
Final depletion	: 1 % U-235
Fuel element discharge	: 30.6. 1979

The position in the reactor, and therefore the exact irradiation history, are unknown.

Firstly, the fuel element was chopped into 3 cm-long pieces (around 4.5 g of Zircaloy each) in the head-end part of the UP-2 plant and the fuel was dissolved using boiling 6M nitric acid. The metallic residues, which had a total volume of 120 litres, were then rinsed batchwise with 13.6 M nitric acid and then with water (around 2,400 l). The hulls were then transferred to six 20 l containers, from each of which a 2 l sample was then extracted. After a further mixing process, the CEA then selected 2 l samples for "Coquenstock 1" and one 2 l sample for PSI. The shearing of the fuel rods also produces small quantities of fine Zircaloy shavings which are deposited on the floor of the dissolver bath together with insoluble fuel particles (e.g. Ru-oxide). The material delivered included practically none of these so-called "fines" and our characterisation was therefore restricted to the actual hull and structural material residues.

3 OVERVIEW OF ANALYSES

3.1 Sampling

One quarter (110 pieces) of the delivered 2 kg of hulls and structural material, corresponding to 528 g, was selected statistically for the overview analyses (RESTANI et al. 1986). 18 pieces or 23 wt-% could be designated as fuel element structural material (spacers, springs, endcaps, etc.) and the remainder was made up of hull fragments.

3.2 Optical evaluation

The hulls are deformed due to the impact of the "chopper" when the fuel elements are being chopped (Figures 1 and 2). Some are compressed or torn apart at the ends.

The remaining structural materials are generally fragmented and partially folded.

Fig. 1: PWR cladding hulls from the UP-2/HAO reprocessing plant.

Fig. 2: PWR cladding hulls; taken from Figure 1 (scale 1:1.2).

3.3 Dose measurement and gamma spectrometry

After a five-year cooling period, the gamma dose rate from the individual Zircaloy fuel rod fragments is between 10 and 40 mR/h (mean 25 mR/h) at a distance of 0.5 m. In the case of the structural components, the activation in the neutron field of the reactor gives rise to a dose which is around a factor of 30 higher and varies widely (Table 1). Gamma spectrometry measurements (Tables 1 and 3) have shown that this coincides with the variations in Co-60 and Mn-54 activities, which again is an indication of the differing contents of Co-59 and Fe-54 in the non-irradiated fuel element structural material.

The Zircaloy hulls are dominated by the fission products and by Sb-125 from the alloying element tin (Table 2). Relatively high fission product activities are also associated with the structural components. Here, the contamination of this material is caused mainly by immersion in the fuel solution, while the fuel rods are already contaminated by fission products in the reactor.

Some nuclide activities were calculated for the cladding waste in order to highlight the significance of the activation products for the overall activity (Table 1).

Table 1: Dose rate and β–, γ-activities of cladding debris (110 pieces, 0.528 kg) from the UP-2 reprocessing of a spent fuel element 5 years after discharge from PWR Obrigheim (burn-up: 30 GWd/tU)

Material	γ-Dose rate at 50 cm and Standard Deviation per sample [mR/h]	Typical Fission Product Activity and Standard Deviation [mCi/kg waste]		Typical Activation Product Activity and Standard Deviation [mCi/kg waste]	
		Cs-137	Ru-106	Co-60	Mn-54
ZIRCALOY-4 (Hulls)	25 ± 8	540 ± 29 % ± 10 %*	460 ± 36 %	64 ± 30 %	3.4 ± 16 %
STAINLESS STEEL INCONEL** (Structure material)	900 ± 750	~ 300 ± 85 %	370	18'500 ± 55 %	325 ± 100 %
CLADDING DEBRIS (73 wt-% Zircaloy-4, 27 wt-% S.S. + Inconel)	(~ 200)	~ 480	~ 440	~ 5'000	~ 90

*: Standard deviation for Cs-137 in dissolved samples for U, Pu-analysis

**: 18 samples

Table 2: Mean fission and activation product activities in Zircaloy-4 hulls 5 years after fuel element discharge from PWR Obrigheim (Germany)

Radionuclide	Average of specific activity and Standard Deviation [mCi/kg Zry-4]
Mn-54	3.4 ± 16 %
Co-60	64 ± 30 %
Ru-106	458 ± 36 %
Sb-125	760 ± 16 %
Cs-134	162 ± 32 %
Cs-137	542 ± 29 %
Ce-144	70 ± 24 %
Eu-154	21 ± 29 %

Table 3: Mean fission and activation product activities in assembly hardware of an irradiated fuel element 5 years after discharge from PWR Obrigheim (Germany)

Radionuclide	Average of specific activity and Standard Deviation [mCi/kg waste]
Mn-54	325 ± 100 %
Co-60	18'500 ± 55 %
Ru-106	370 ± 65 %
Cs-137	300 ± 85 %

3.4 α-autoradiography

α-autoradiography using solid state nuclear track detectors (SSNTD) was used to assess the qualitative transuranic activity distribution on the Zircaloy hull surfaces (RESTANI & MÜLLER 1987). The hulls were cut lengthwise and the α-sensitive films were pressed onto the surface using a pneumatically operated stamping apparatus. The emission of α-particles caused tracks of disturbance in the cellulose nitrate film material; these damage tracks could be made visible by etching.

The Zircaloy hulls are completely contaminated both inside and outside, although the contamination is generally inhomogeneous. On the outermost surface layer of the inside, there are often very high local α-activities (Figures 3 and 5) which are visible with a periscope as actual deposits (Figures 6-8). These highly concentrated fuel residues are often present as loose contamination which can at least be reduced by repeated contact with the cellulose nitrate film.

Once the "hot spots", which obscure the background contamination, have been eliminated (cf. Figure 3), special features of the fuel column which were transferred to the surface become visible (JENKINS I.L. et al. 1982; RESTANI & MÜLLER 1987). Three circumferential intermittent lines from fuel pellet boundaries caused by abrasion are shown in Figure 4, at regular intervals of 11 mm. The α-depleted axial lines mark scratches which run along the pellet surfaces and could have been caused before irradiation.

The structure of the α-activity distribution is not necessarily the same in the two halves of the hull. If one half is more strongly contaminated than the other, it is possible that dissymetry of fuel solution deposits is the explanation.

The distribution pattern often resembles that in Figure 5, with randomly distributed, high α-concentrations. Extensive deposits of fuel and optically more or less blank inner surfaces are both fairly rare. Hull deformation also appears to be partly responsible for determining the degree of contamination since it affects the cleaning process during rinsing (Figure 8).

The outer surface of the Zircaloy hulls has large, more closely associated areas of even contamination. The patterns show a smearing effect, which fits with the theory that the contamination on the coolant side is caused by deposition processes during fuel dissolution. On the fuel side, there are also some residues of insufficiently rinsed or undissolved fuel, corrosion products of the Zircaloy-fuel interaction and small amount of fissile material embedded in the ZrO_2 layer by recoil processes during fission, and by thermal diffusion (JENKINS et al. 1982; GUÉ et al. 1987).

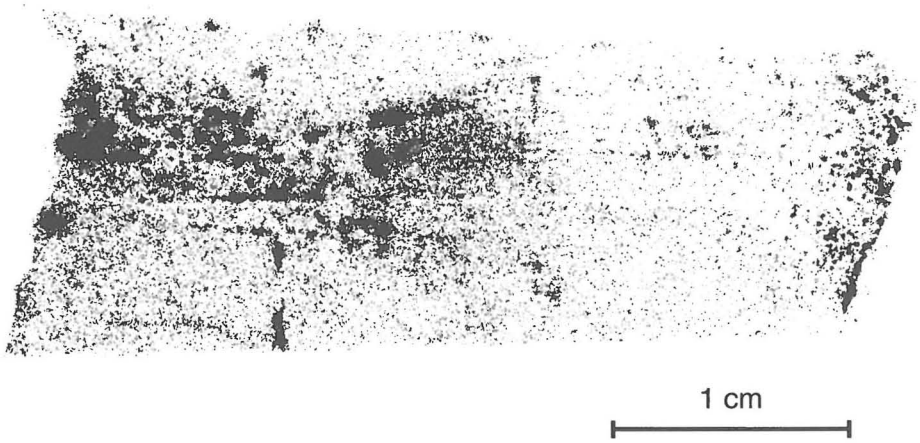

Fig. 3: α-autoradiograph of the inside of a halved Zircaloy hull. 1st exposure, 10 s exposure time, hot spots left and right.

Fig. 4: α-autoradiograph of the inside of a halved Zircaloy hull (same hull as in Figure 3). 5th exposure, 20 s exposure time; hot spots practically removed by successive exposures.

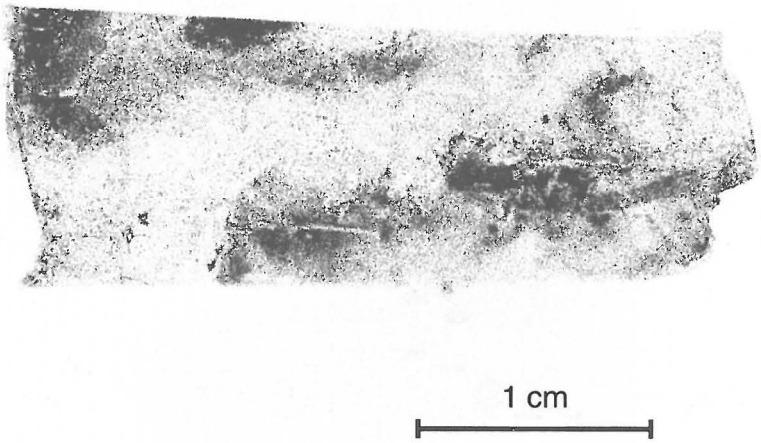

Fig. 5: α-autoradiograph of the inside of a halved Zircaloy hull. Local areas with high α-concentration.

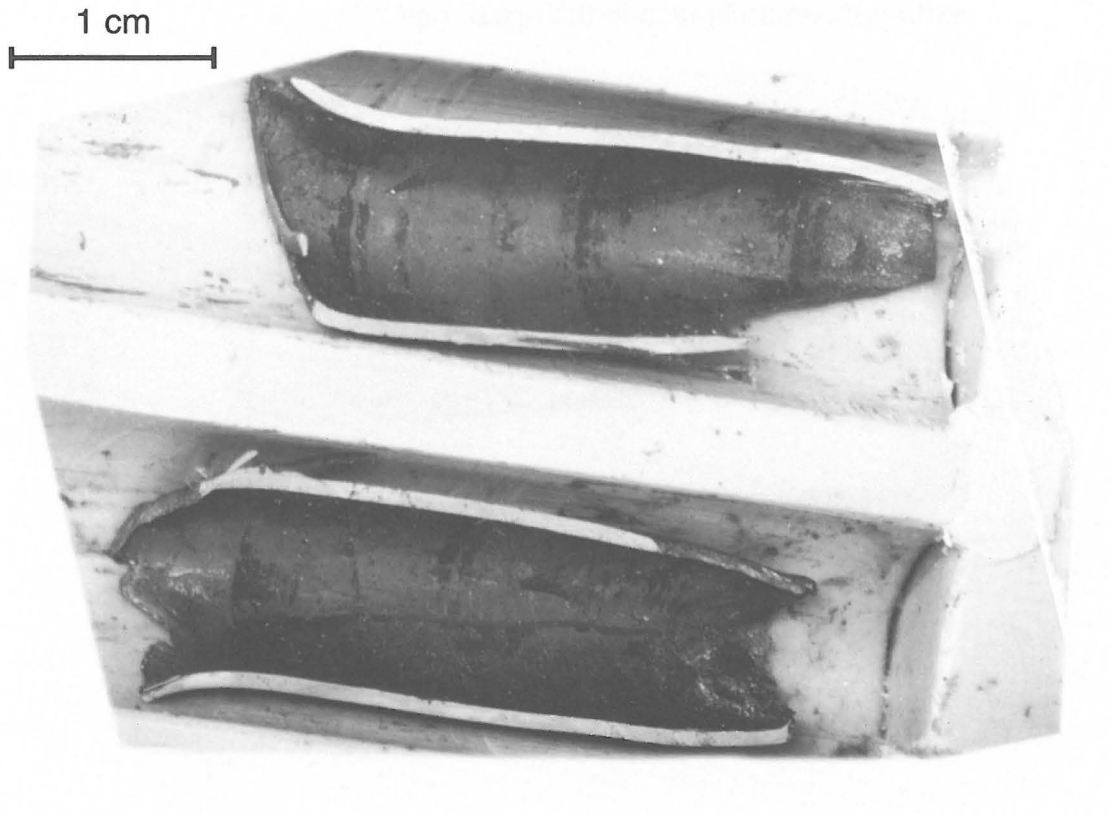

Fig. 6: Periscope image of the inside of a Zircaloy hull cut lengthwise. Contamination traces of the pellet boundaries at regular distances of 11 mm. The lower half is more strongly contaminated, with a larger deposit visible at the right end of the hull.

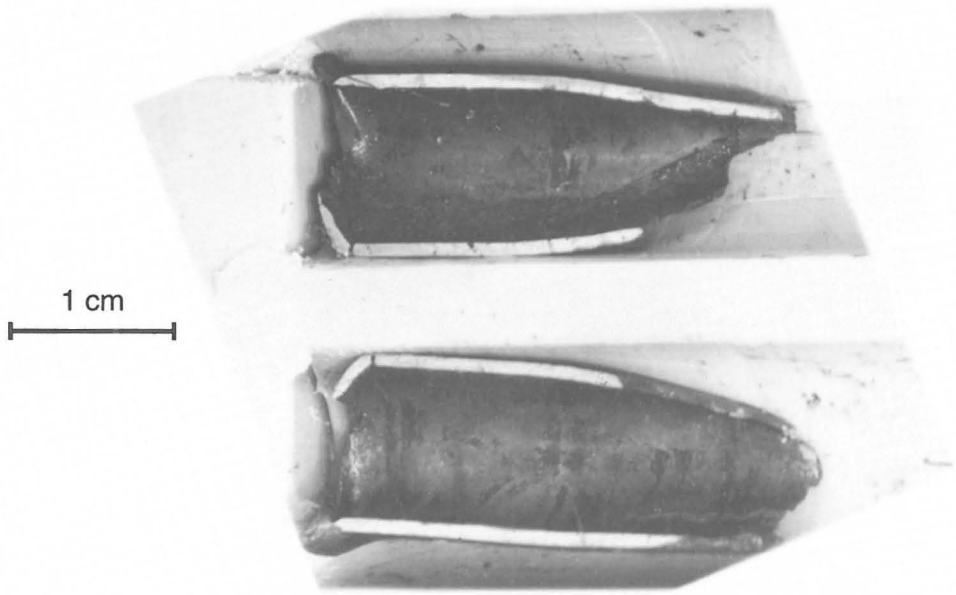

Fig. 7: Periscope image of the inside of a Zircaloy hull (two halves). Axial extent of contamination in the upper half.

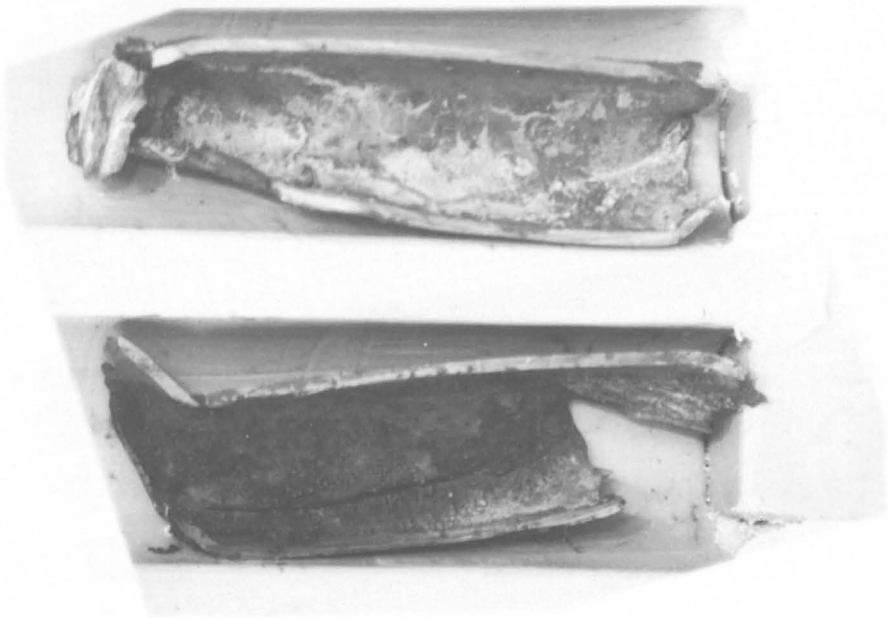

Fig. 8: Periscope image of a strongly contaminated Zircaloy hull. One end was compressed and practically sealed.

4 ACTINIDE ANALYSIS OF ZIRCALOY HULLS

The actinide contents of the Zircaloy-4 hulls were measured using isotope dilution analysis and α-spectrometry after dissolution of individual samples in 3M HNO_3/2M HF. These methods are described in detail in the Appendix to this report.

4.1 Isotope dilution analysis of uranium and plutonium

From each sample analysed, two Zircaloy sample solutions were taken and one loaded with the spikes U-233 and Pu-242. Uranium and plutonium were separated as nitrate complexes by means of anion-exchange columns. For this purpose, plutonium was converted to the tetravalent oxidation state using $NaNO_2$, while the uranium remained in its hexavalent state. The differing stability of the nitrate complexes was of use in the elution with nitric acid from the anion exchange columns. The elements separated in this process were purified using further ion-exchangers and prepared for mass spectrometry (MS) by vapourising the sample solutions on rhenium bands. The mass ratios of the spiked and unspiked uranium and plutonium samples obtained by MS were then converted according to the dilution principle into effective amounts of isotopes.

The results are presented in Tables 4 and 5. In order to obtain an impression of the distribution of U and Pu contamination, single Zry samples were first investigated. As determined from the results of the optical characterisation and α-autoradiography, the U- and Pu-contents vary widely, between 380 and 2,130 mg U/kg Zry and 6.3 and 25.3 mg Pu/kg Zry. Particularly in the case of hulls whose ends are half-closed or are otherwise strongly deformed, higher α-concentrations can be measured. This is because fuel inclusions are more easily formed in such cases. The Cs-137 activities of the same samples do not vary so markedly and, if they are plotted against uranium (Figure 9), only a tendency towards a linear correlation can be seen (correlation coefficient < 0.6). As will be discussed later (section 6), the reason for this is that contamination with fission products is to some extent different to that with fissile material. Cs-137 is therefore poorly suited as a reference nuclide for residual uranium and plutonium when characterising cladding waste. On the other hand, there is a moderately constant U/Pu weight ratio between these two actinides of 85:1 (Figure 10); the mean concentrations five years after ceasing irradiation are 1,130 mg U/kg Zry and 13.6 mg Pu/kg Zry.

Table 4: Uranium-plutonium concentrations and isotopic compositions in Zircaloy-4 hulls after 5 years cooling time.
Results of isotope dilution mass spectrometry

Number of hulls/ Sample No.(1)	Weight [g]	Uranium [mg U/kg Zry]	U-234 [wt-%]	U-235 [wt-%]	U-236 [wt-%]	U-238 [wt-%]	Plutonium [mg Pu/kg Zry]	Pu-238 [wt-%]	Pu-239 [wt-%]	Pu-240 [wt-%]	Pu-241 [wt-%]	Pu-242 [wt%]
1/23	3.74	1242	0.031	1.21	0.40	98.36	12.6	1.27	61.25	22.77	10.26	4.45
1/80	4.37	423	0.023	1.17	0.38	98.43	6.3	1.33	60.74	23.15	10.18	4.59
1/87	4.15	1410	0.026	1.18	0.39	98.41	14.2	1.35	60.88	23.16	10.13	4.49
1/67	4.30	1201	0.024	1.17	0.38	98.43	14.9	1.34	61.02	23.13	10.14	4.38
1/33	4.31	2127	0.026	1.17	0.39	98.41	25.3	1.38	60.92	23.29	10.04	4.38
1/93	4.66	376	0.031	1.19	0.39	98.39	6.3	1.33	60.97	23.07	10.15	4.48
1/85	3.67	1095	0.026	1.19	0.39	98.40	12.1	1.32	61.04	22.98	10.15	4.51
1/75	3.67	786	0.020	1.22	0.36	98.41	9.2	1.28	61.12	22.86	10.14	4.60
1/121	6.00	956	0.023	1.15	0.39	98.44	7.3	1.37	60.40	23.16	10.37	4.70
1/101	4.61	756	0.026	1.13	0.39	98.45	14.4	1.40	60.27	23.38	10.28	4.68
5	23.10	1234	0.024	1.21	0.37	98.40	16.0	1.31	61.36	23.04	9.94	4.35
5	16.16	1600	0.030	1.22	0.38	98.37	21.5	1.33	61.35	23.09	9.92	4.31
5	16.96	419	0.023	1.16	0.38	98.44	7.6	1.33	60.59	23.21	10.23	4.63
6	17.78	1468	0.021	1.17	0.39	98.42	12.4	1.35	61.04	23.18	10.01	4.41
Average quantities		1132 ±446(2)	0.025	1.19	0.38	98.41	13.6 ±5.0(2)	1.33	61.01	23.12	10.08	4.46
1/73 (cleaned)	4.05	41(3)					2.1 (3)					

(1) Sample Number as allocated in (RESTANI et al. 1986)

(2) Standard deviation

(3) Residual amounts of U and Pu after cleaning with 6N nitric acid in an ultrasonic bath for 15 minutes.

Taking into account the standard deviation, it can be seen that there is a good agreement with the value of 10.7 mg Pu/kg cladding (GUÉ et al. 1987, Table III.5) determined by passive neutron measurement for the whole cladding delivery. In these 2 kg of cladding there are also structural components of the fuel element bundle. These were only contaminated with α-activity by secondary contamination in the fuel dissolver (cf. also section 3.3). It can be assumed that they are less contaminated with undissolved fuel and that the actinide concentrations are therefore not higher than in the Zircaloy hulls (cf. measurements in JENKINS I.L. et al. 1982; GUÉ et al. 1987). The elements Pu, Am and Cm can deviate from this pattern since they are deposited in solution on surfaces as slightly hydrolysable ions. In the tetravalent state, Pu also shows a marked affinity for oxidic surfaces. Local increases in pH in near-surface areas lead then, even in an acidic environment, to Pu absorption (JENKINS et al. 1982).

Table 5: Activities of Plutonium isotopes in Zircaloy-4 hulls after 5 years cooling time.
Results of isotope dilution mass spectrometry (in mCi/kg Zry)

Number of hulls/ Sample No.(1)	Pu-238	Pu-239	Pu-240	Pu-242	Total Pu(α)	Pu-241
1/23	2.72	0.48	0.65	0.0022	3.85	133
1/80	1.42	0.24	0.33	0.0011	1.99	66
1/87	3.26	0.54	0.74	0.0025	4.54	148
1/67	3.41	0.57	0.78	0.0026	4.75	155
1/33	5.96	0.96	1.34	0.0044	8.26	262
1/93	1.43	0.24	0.33	0.0011	2.00	66
1/85	2.74	0.46	0.63	0.0021	3.83	126
1/75	2.01	0.35	0.48	0.0017	2.84	96
1/121	1.71	0.28	0.38	0.0014	2.38	78
1/101	3.44	0.54	0.77	0.0027	4.75	153
5	3.59	0.61	0.84	0.0027	5.03	164
5	4.90	0.82	1.13	0.0036	6.86	220
5	1.73	0.29	0.40	0.0014	2.41	80
6	2.86	0.47	0.65	0.0021	3.98	127
Mean Pu(α) activity					4.32	

(1) Sample number as allocated in (RESTANI et al. 1986)

The following discussion is intended to analyse the origin of the inner hull surface contamination:

The first argument for only a small contribution from the remaining undissolved fuel is the following one. The U- and Pu-isotopic compositions are constant for the investigated individual hulls and independent of the degree of contamination (Table 4). These compositions also correspond to the data for the bulk hull material (GUÉ et al. 1987). The axial burn-up distribution in the reactor is, according to information from Obrigheim's staff, not particularly flat (form factor[1]=1.15). The ORIGEN calculation with only a 7 % deviation from the mean burn-up of 30 GWd/tU already results in a distinctly different U- and Pu-isotopic composition. If the remaining adherent fuel activity would be more important than the fuel solution deposit activity, a significant variation in both U- and Pu-isotopic compositions would be expected. However as the number of samples examined was small, this argument is not absolutely conclusive. Furthermore, the secondary contamination from dissolved fuel, which clearly affects the outer hull surface, attenuates the expected isotopic variations.

The second argument is based on the radial distribution of the Pu-isotopic composition in the fuel calculated by EDF[2] for the known burn-up and enrichment. The calculations take account of the epithermal nuclear reaction and the higher burn-up at the pellet rim and therefore give the values for undissolved, adherent fuel on the inner hull surface. According to these calculations, the Pu-238 and Pu-240 isotopic contents should be lower, and the Pu-241 and Pu-242 contents higher, than for the fuel solution (GUÉ et al. 1987, Table IV.3) and for the contaminated cladding of this work. As this is not the case, it can be derived that the remaining fuel contamination is relatively small.

The third argument is based on the values measured for the U/Pu-ratio which were found to be constant. If significant quantities of undissolved fuel were remaining, this constant ratio would not have been expected for the same reasons given for the first argument. However, as a result of the experimental insensitivity (correlation factor: 0.88), this is not considered to be conclusive. Furthermore, as a result of the secondary contamination, the preferential Pu absorption out of the solution on to the hull surfaces (GUÉ et al. 1987) decreases and distorts the specific characteristics of the undissolved fuel contamination. (The preferential Pu absorption leads to clearly lower U/Pu ratios for the hulls and the structural materials than for the fuel solution (GUÉ et al. 1987)).

It is not considered possible to confirm a direct link between local burn-up and the degree of contamination from undissolved fuel. If this link exists, it must be demonstrated by the examination of a fuel element which has been in operation to a much higher level of burn-up.

In order to summarise, it is concluded that the fuel dissolution process was efficient (low residual undissolved fuel contamination) and the secondary contamination by the fuel solution was relatively significant (the overall contamination of the hulls and the structure materials are comparable even though the structural materials have not been in contact with undissolved fuel). The rinsing of the hulls after dissolution could be further improved.

---

(1) Axial form factor = ratio of maximum to mean axial burn-up

(2) Electricité de France, Clamart

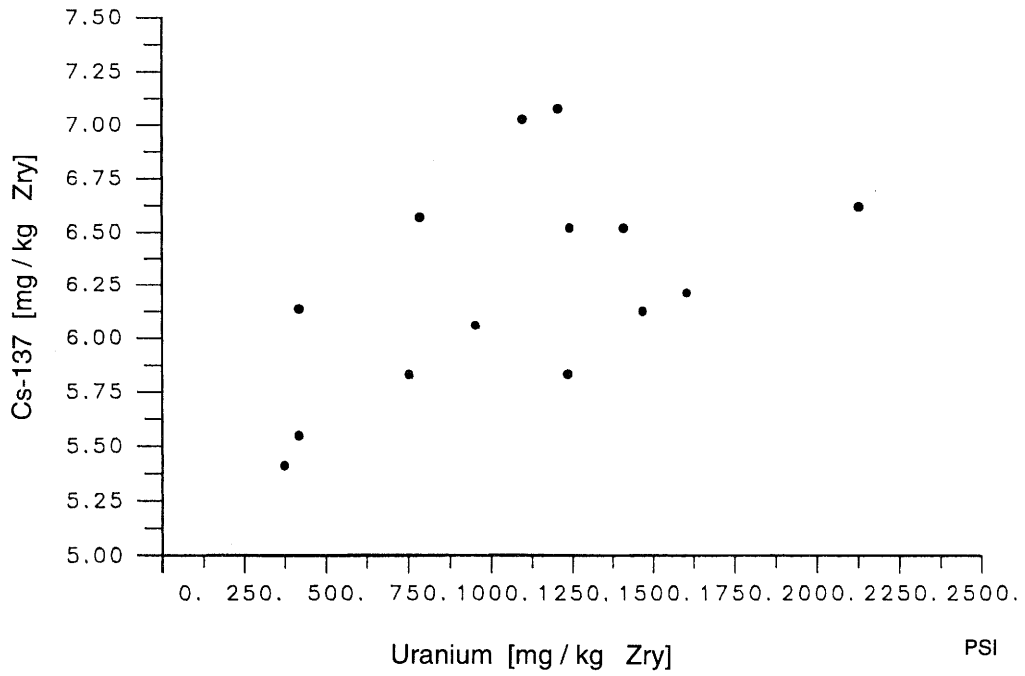

Fig. 9: Cs-137/uranium ratio in PWR Zircaloy hulls (5 years after discharge).

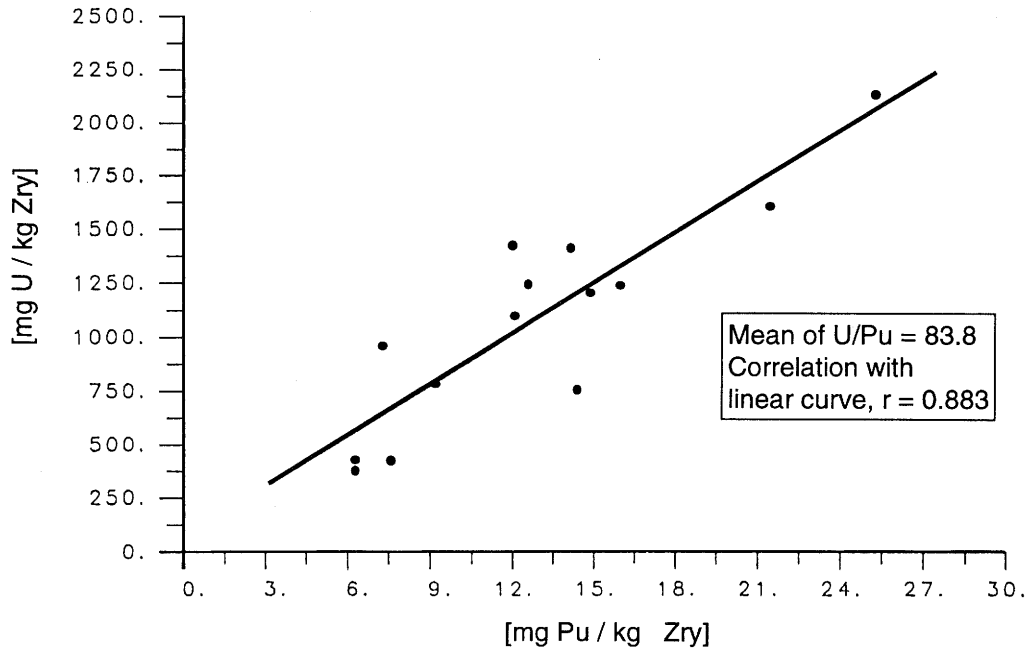

Fig. 10: Uranium/plutonium ratio in PWR Zircaloy hulls (5 years after discharge).

4.2 α-spectrometry

Aliquots of the Zircaloy solutions to be measured were mixed with tetraethyleneglycol (TEG) and vapourised on a rotating, stainless steel plate. After heating in an oven, the preparates were measured by recording the α-spectrum using a silicon surface barrier detector.

The total alpha activity was measured after 50-times dilution of the original Zircaloy solution.

For α-spectrometry of Am-241, plutonium had to be separated out because of the peak overlap with Pu-238. The extraction of the tetravalent plutonium was done either with trioctylamine (TOA) or thenoyltrifluoroacetone (TTA). The aqueous phase with the trivalent americium and curium was vapourised and the sample dissolved in nitric acid. One aliquot was then taken from this solution for α-spectrometry.

The detailed results are presented in Table 6 for 8 1/3 year cooling as well as the average values for the reference 5 year cooling time. After a five-year cooling time, 0.9 mCi Am-241/kg Zry and 1.25 mCi Cm-244/kg Zry were measured. The total α-activity after the same time period is 6.7 mCi/kg Zry (= 250 MBq/kg Zry). The difference gives a Pu(α) activity of 4.5 mCi/kg Zry. This value agrees very well with the results from the more accurate isotope dilution analysis. Small amounts of Am-243 and Cm-242 are included in the activity concentrations of Am-241 and Cm-244. In the α-spectrum, Am-243 disappears in the "low energy tail" of the Am-241 and could no longer be detected using this preparation technique. The Cm-242 activity is always below 0.1 mCi/kg Zry.

4.3 Neptunium neutron activation analysis

Np-237 can be analysed following irradiation with thermal neutrons by measuring the 984 keV gamma line of the generated Np-238 (DEGUELDRE C.A. 1984).

In order to rule out potential disturbing effects on the gamma spectrometry and therefore on the sensitivity of the method, the fission products and uranium and plutonium were removed from the solution. This was done by extracting the oxidised, hexavalent uranium, plutonium and neptunium using methylisobutyl-ketone and then the reduced tetravalent neptunium using TTA/Xylene. The isolated neptunium was irradiated in sealed glass ampoules.

Before the TTA extraction there are two critical steps in the procedure which restrict the total yield to around 70 %. The result of 250±95 nCi Np-237/kg Zry (= 355 ppb) therefore contains an element of uncertainty which could be as high as 20 %.

Table 6: Alpha activities in Zircaloy-4 hulls.
Results of α-spectrometry (in mCi/kg Zry)

Number of hulls/ Sample No.	Total α	Am-241	Cm-244	Pu(α)	Pu(α) (Mass Spectrometry)
8 1/3 year cooling time					
1/80	3.32	0.82	0.57	1.93	1.96
1/87	6.67	1.58	1.10	3.99	4.48
1/67	6.92	1.48	0.96	4.48	4.69
1/33	13.8	3.16	2.28	8.35	8.15
1/93	3.13	0.75	0.51	1.87	1.97
1/85	6.25	1.51	1.12	3.62	3.77
1/75	4.95	1.24	1.13	2.58	2.79
1/121	5.52	1.74	1.54	2.24	2.32
1/101	6.60	1.44	0.90	4.26	4.67
5	8.10	1.67	0.98	5.45	4.95
5	11.6	2.54	1.67	7.40	6.73
5	3.65	0.85	0.55	2.25	2.37
6	6.80	1.49	1.16	4.15	3.76
Average:	7.19	1.61	1.11	4.47	4.29
Standard deviation:	±2.71	±0.56	±0.36	±1.85	±1.55
Weighted average:	7.10	1.59	1.09	4.42	4.23
5 year cooling time					
Average:	6.74	0.92	1.26	4.56	4.37
Weighted average:	6.65	0.90	1.24	4.51	4.32

5 CLEANING OF ZIRCALOY HULLS

A few of the hulls with average beta,gamma activity were cleaned for 15 minutes in an ultrasonic bath with 6M nitric acid.

As a result, the fission product activity decreased between 10 and 40 % depending on the nuclide (RESTANI et al. 1986).

One hull was checked for residual U- and Pu-content. The loosely bound alpha contamination (cf. section 3.4) was largely removed and, particularly in the case of uranium, resulted in a very low residual contamination of 40 ppm (Table 4). Comparing with the mean U-, Pu-content of the hulls, the experiment shows that there is great potential for α-removal by an appropriate cleaning process (see also GUÉ et al. 1987).

6 SIMS DEPTH PROFILE ANALYSIS

A shielded secondary ion mass spectrometer was available for making qualitative measurements of near-surface concentration depth profiles of active samples. This method involves eroding the sample surface by bombardment with primary ions. The impact processes induced by this give rise to an emission of secondary ions which is characteristic for the chemical composition of the sample. These atomic and molecular secondary ions are separated according to mass in a quadrupole mass spectrometer.

The SIMS depth profiles presented in Figures 11 to 15 are the result of bombardment of Zircaloy surfaces with O_2^+ ions. The secondary ion intensities depend on several parameters, including the atomic number and the material bombarded (the curves shown do not give the mol ratios).

In Figure 11, the initially differing trends between the Zr secondary isotope masses 90 and 94 and the ZrO^+ of isotope masses 106 and 108 are a measure of the oxide layer thickness at this location. After around 1-2 µm, the primary beam seems to have broken through this layer on the inside since the ion intensity ratios remain more or less constant from this point on.

It can be seen in Figure 12 that a considerable proportion of the fission products is implanted as recoil particles in the inner surface. Sr-88, which is the lightest of the fission nuclides investigated, as expected penetrates furthest (around 12 µm) into the surface. Cs-137 reaches a penetration depth of around 10 µm; a similar value was measured by KfK (VEHLOW J. 1985), by determining the release of activity in a corrosive solution as a function of wall erosion. The marked similarity in trend for caesium isotopes with masses 133 and 137 (Figure 13) shows that the diffusion behaviour of the element also plays a certain role in migration. The trend of the uranium concentration was also included in Figure 13 with UO^+ as the detected secondary ion. The marked drop in concentration on the inner surface shows that the majority of the uranium is deposited on the oxide layer, but also emplaced within it. Similar behaviour is expected for the other actinides, which were not measurable.

Successful cleaning, as mentioned in section 5 and tested in detail (GUÉ et al. 1987), is therefore much more likely for uranium, which is directly exposed to the cleaning fluid, than for the fission products.

The different contamination pathways of the actinides and the fission products on the inner surface of the hulls shown by this method are also the reason for the lack of correlation between uranium and caesium (cf. section 4.1).

The thickness of the oxide layer on the outer surface is around 7-8 µm (Figure 14). The concentration trends of uranium and the fission products agree well in this case (Figure 15) and therefore confirm the assumption that contamination arises due to deposition in the fuel dissolver (cf. section 3.4). All the nuclide concentrations decrease rapidly as one moves from the surface into the oxide layer and show the same pattern as uranium on the inner surface.

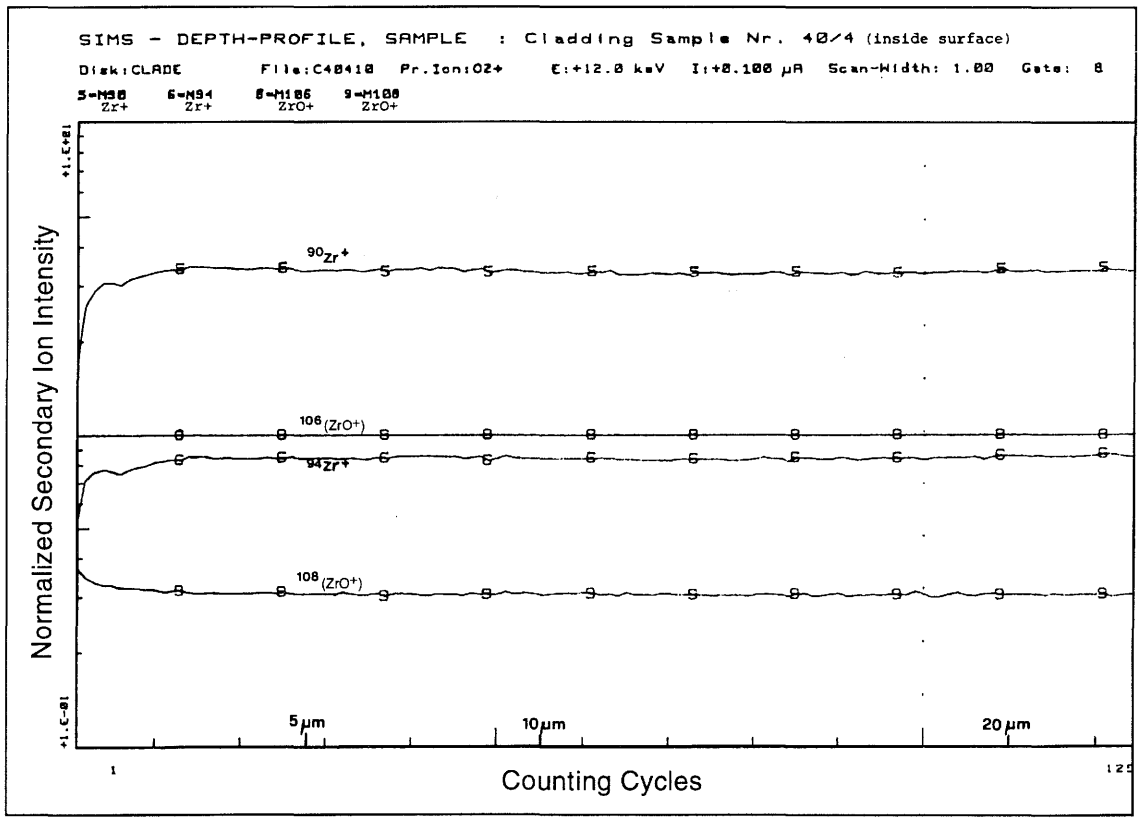

Fig. 11: SIMS depth profile on the inside of a Zircaloy hull. Intensities normalised to mass 106 (ZrO^+). Differing trends of the Zr^+ to ZrO^+ intensities are a measure of the oxide layer thickness (around 1-2 µm).

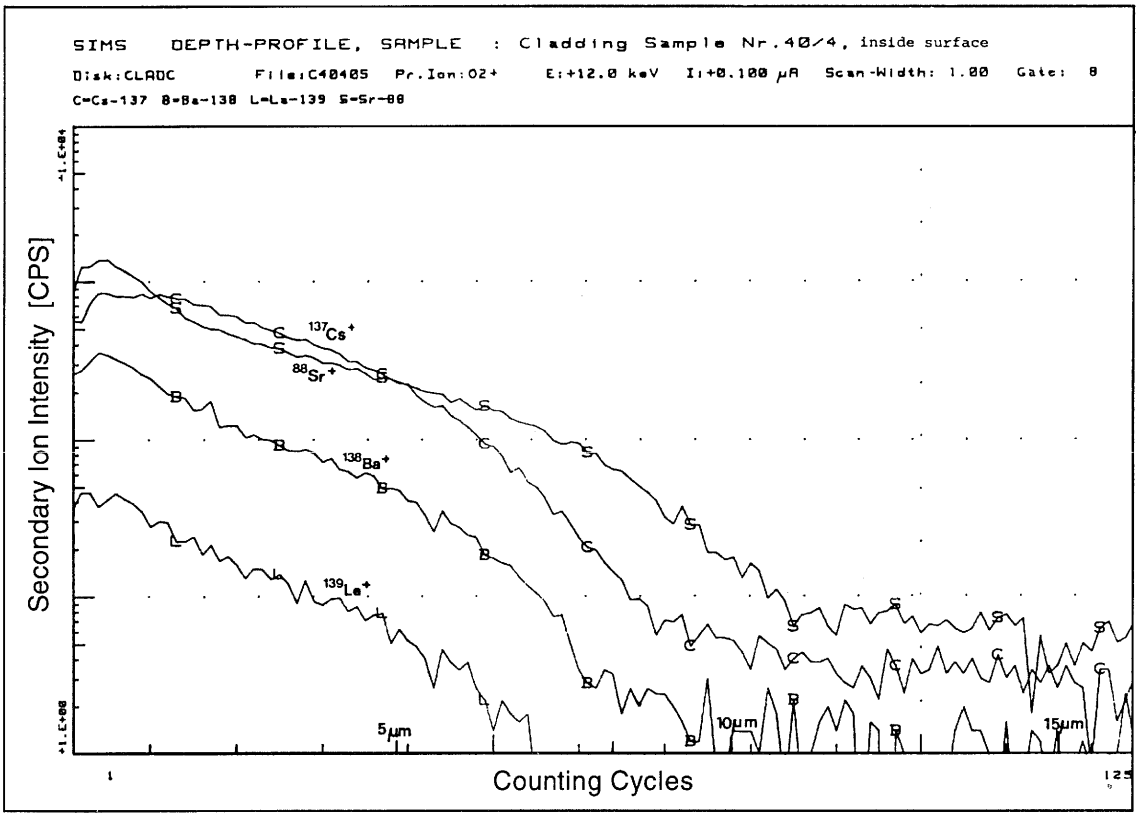

Fig. 12: SIMS depth profile on the inside of a Zircaloy hull. Fission product intensities vs. surface depth.

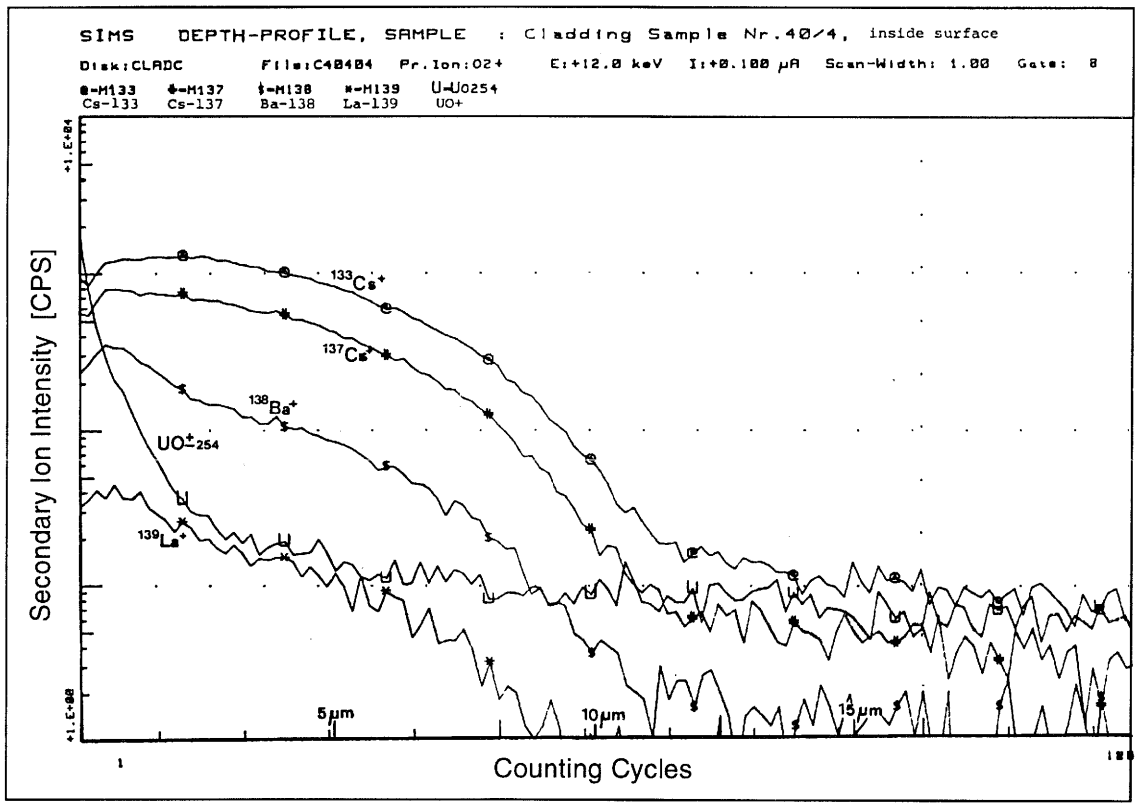

Fig. 13: SIMS depth profile on the inside of a Zircaloy hull. Uranium concentration compared to the fission products.

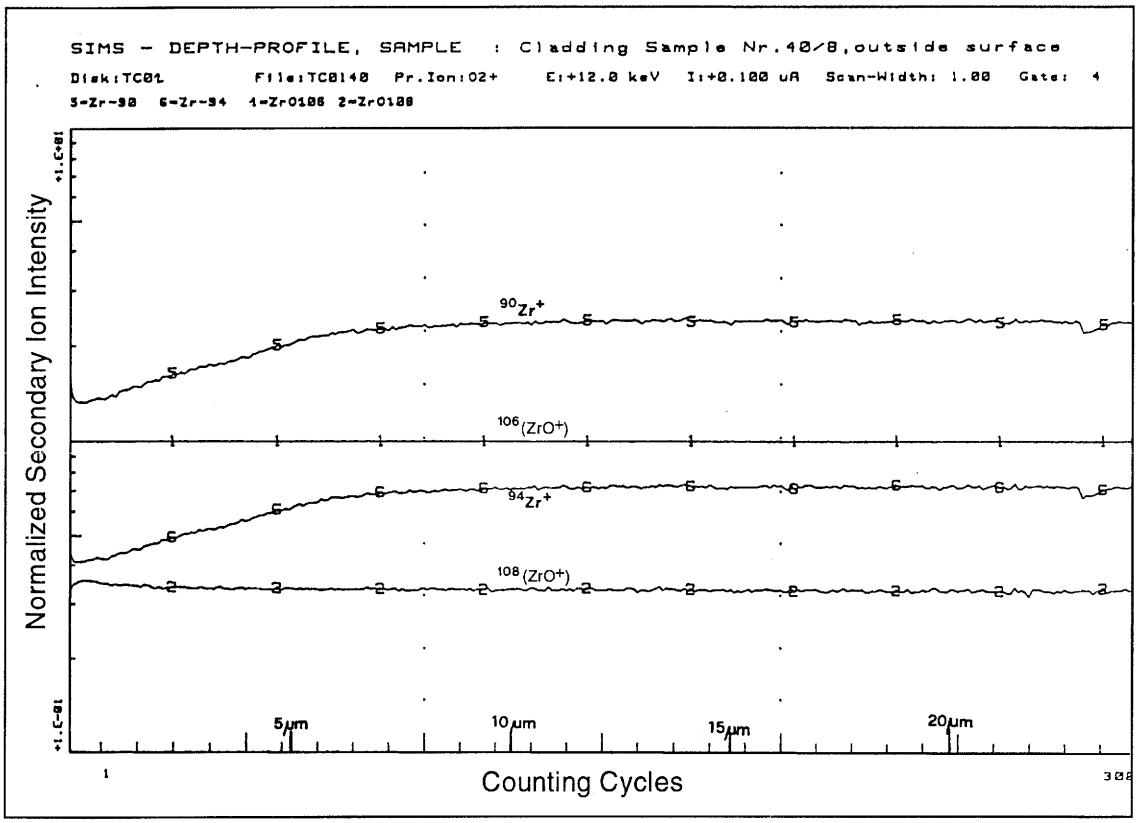

Fig. 14: SIMS depth profile on the outside of a Zircaloy hull. Oxide layer thickness around 7-8 µm.

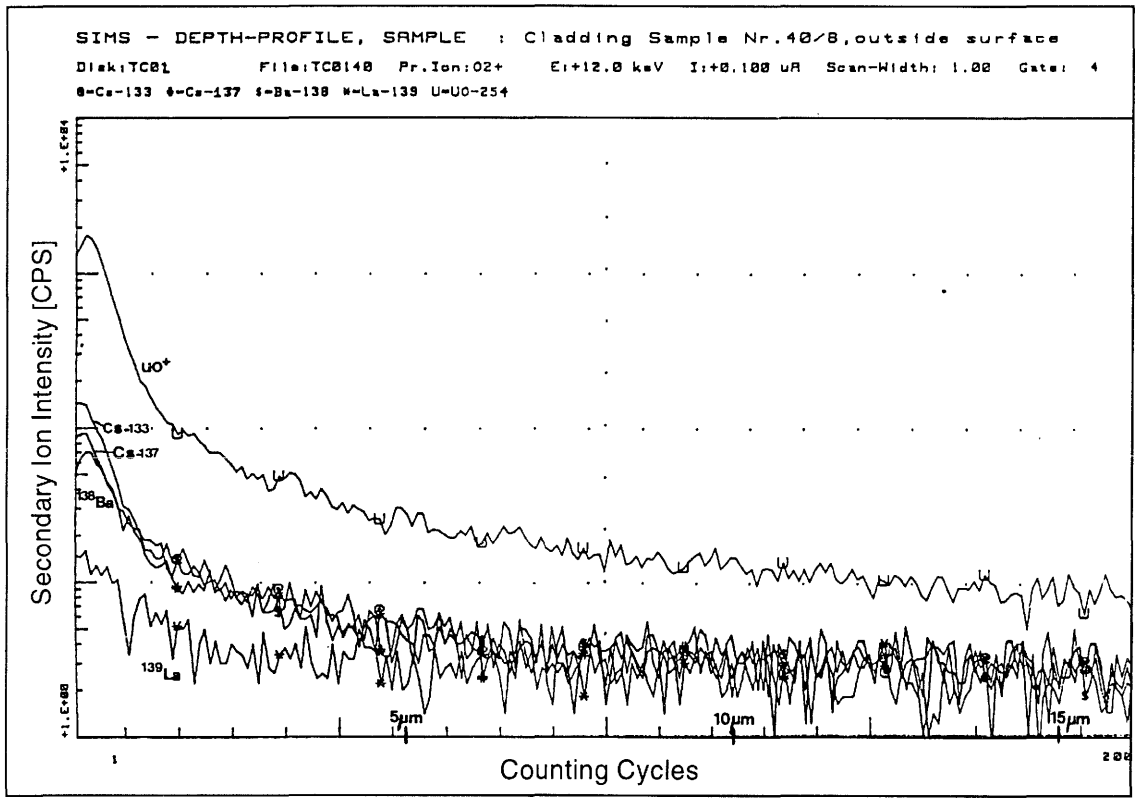

Fig. 15: SIMS depth profile on the outside of a Zircaloy hull. Uranium concentration compared to the fission products.

7 SURFACE STRUCTURE ANALYSIS OF ZIRCALOY FUEL ELEMENT HULLS

7.1 Oxide layer analysis

A thin, protective oxide layer builds up on newly produced Zircaloy fuel rods. This gives the material an excellent corrosion resistance. The oxide layer is then further extended by oxygen uptake on the coolant side of the hull. Further oxide build-up is also possible on the fuel side during irradiation through reaction with UO_2. Layer thicknesses of 6.5 to 11 µm (Figures 16, 17) were measured on the outside, with the values for the inside generally being between 1 and 2 µm (Figures 20-22). At some isolated locations, the ZrO_2 layer grew to a thickness of around 8 µm (Figures 18, 19, 23), which could partly be due to the effect of acid attack in the dissolver on the damaged surface.

During the interaction with the Zircaloy surface, the reduced uranium is also dissolved and forms a metallic, uranium-rich U/Zr alloy in the oxide layer and in the α-Zr(O) (MALLETT et al. 1957; GROSSMAN et al. 1965; HOFMANN et al. 1984). However, because of low reaction and diffusion rates under reactor conditions, the amounts will be small (MALLETT et al. 1957). α-emitters can also be implanted in the oxide layer due to collision with heavy fission fragments. The range decreases exponentially with depth and should be a maximum of 1 µm (JENKINS et al. 1982). The amount depends to a large extent on the conditions at the fuel/cladding phase boundary (gap, fission gas, etc.) and could vary by orders of magnitude.

The assumption that the rough oxidised inner and outer surfaces present a good base for radioactive deposits from the leaching bath is more certain (cf. section 7.2). Hydrolysed transuranic ions in particular tend towards deposition on oxidic surfaces (JENKINS et al. 1982). Once absorbed, the activity is no longer easily removed in the nitric acid solution since the oxide layer and the associated colloidal species are hardly affected.

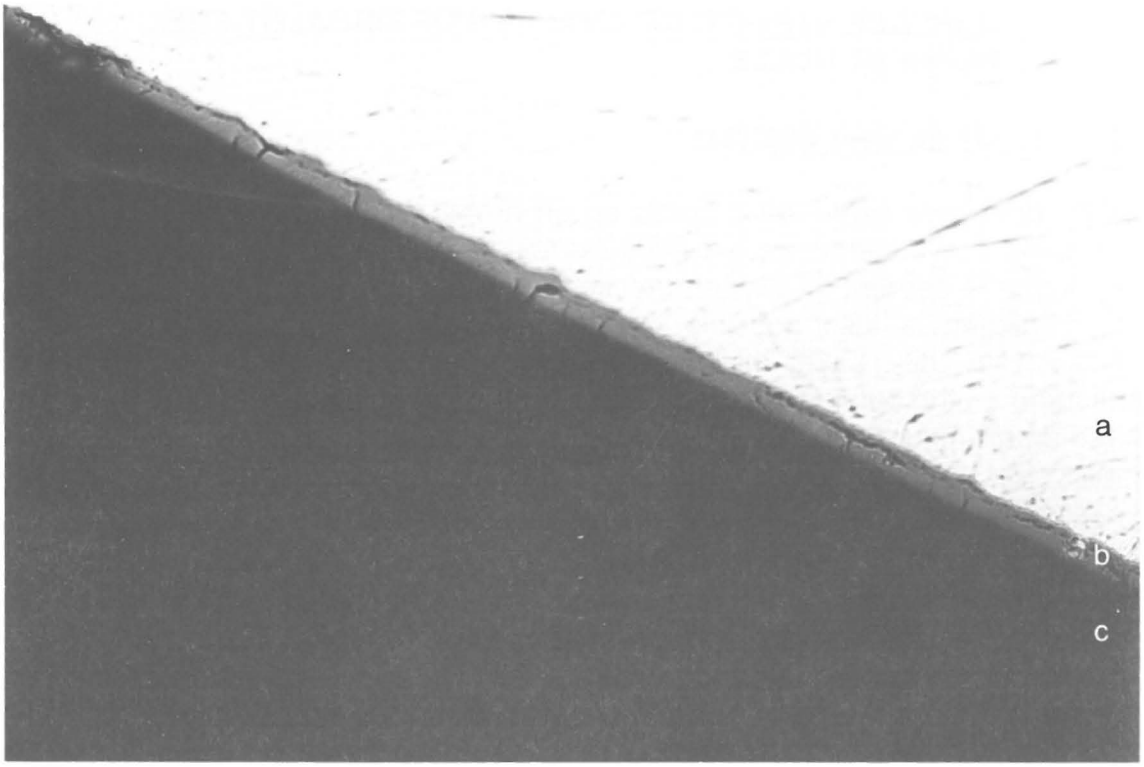

Fig. 16: Metallographic image of a Zircaloy-4 hull cross-section (magnification 500x). Normal ZrO_2 layer on the outside.
a: Zircaloy-4, b: Zirconium oxide, c: embedding material.

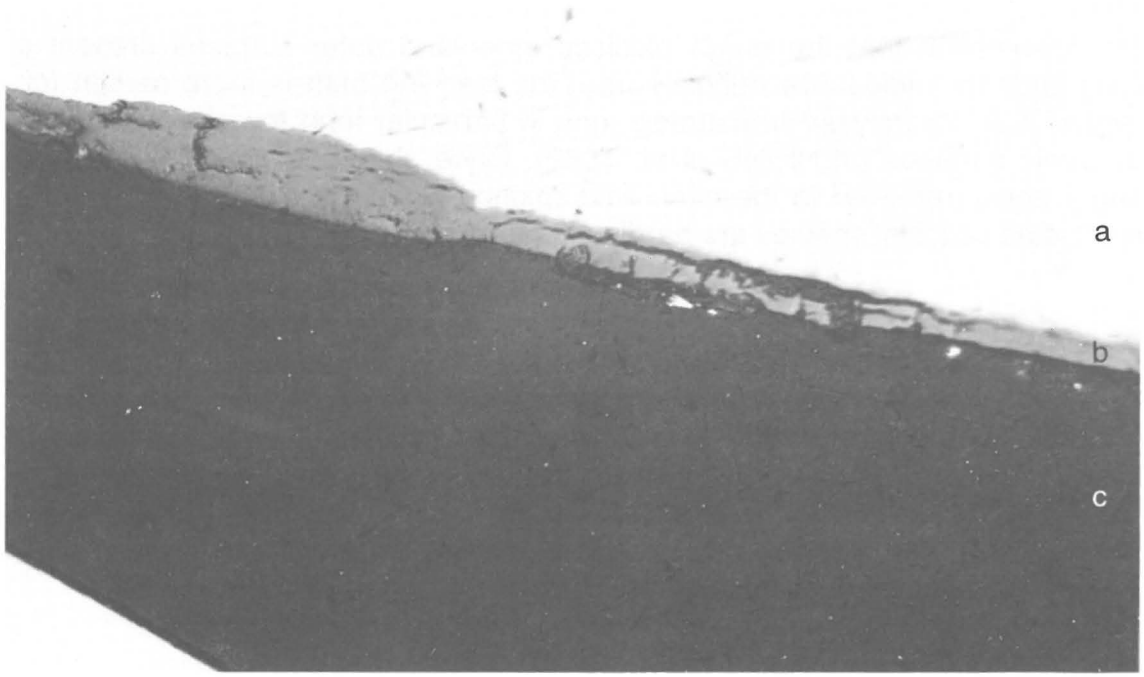

Fig. 17: Locally increased oxide layer formed on the outer surface (magnification 500x).
a: Zircaloy-4, b: Zirconium oxide, c: embedding material.

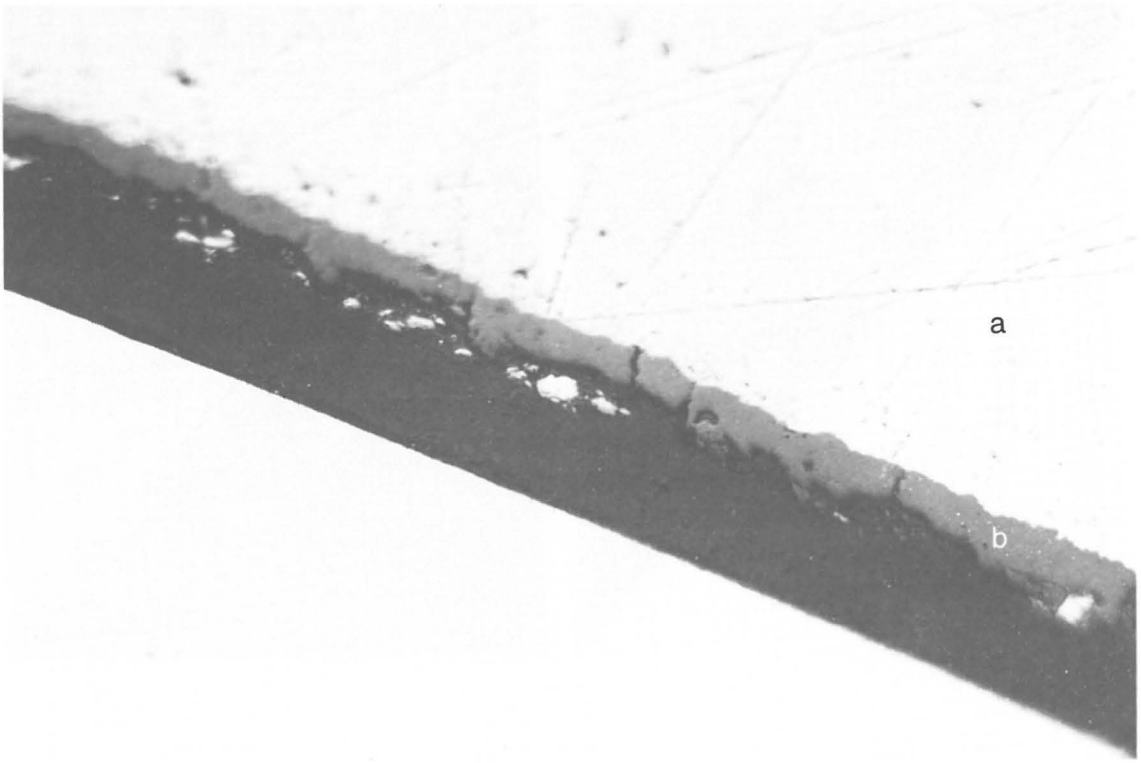

Fig. 18: Metallographic image of a Zircaloy-4 hull cross-section (magnification 500x). Oxide layer on the inside.
a: Zircaloy-4, b: Zirconium oxide.

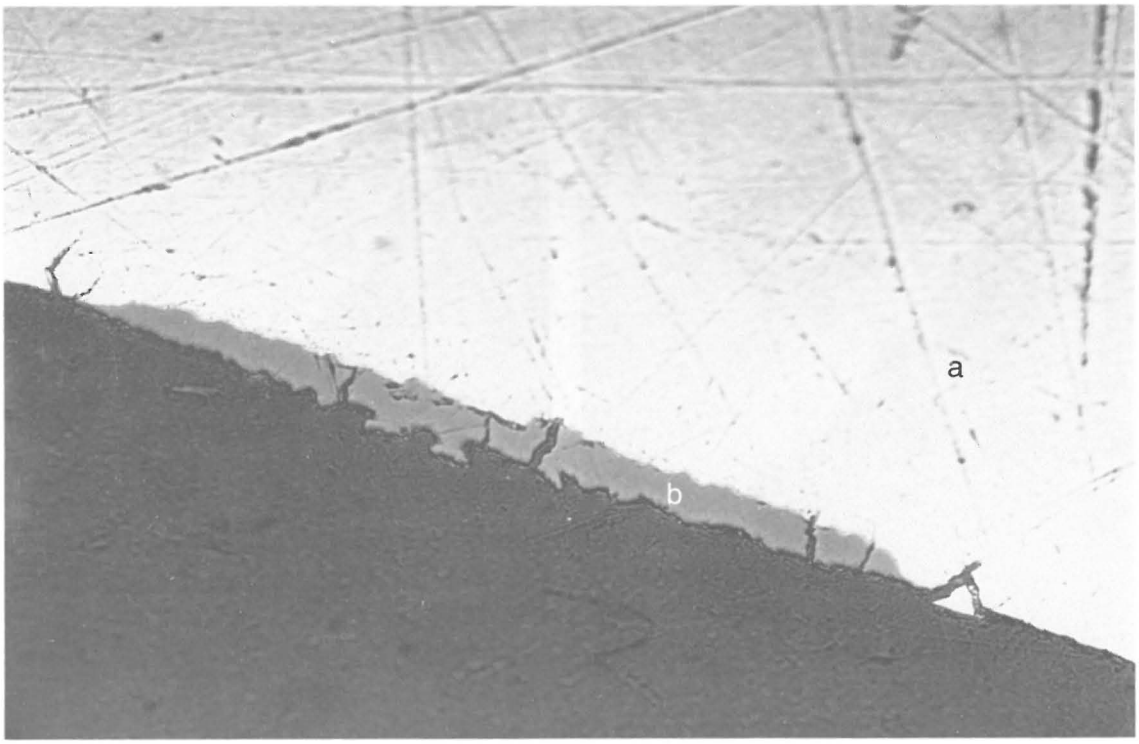

Fig. 19: Locally increased oxide formation on the inside (magnification 500x).
a: Zircaloy-4, b: Zirconium oxide.

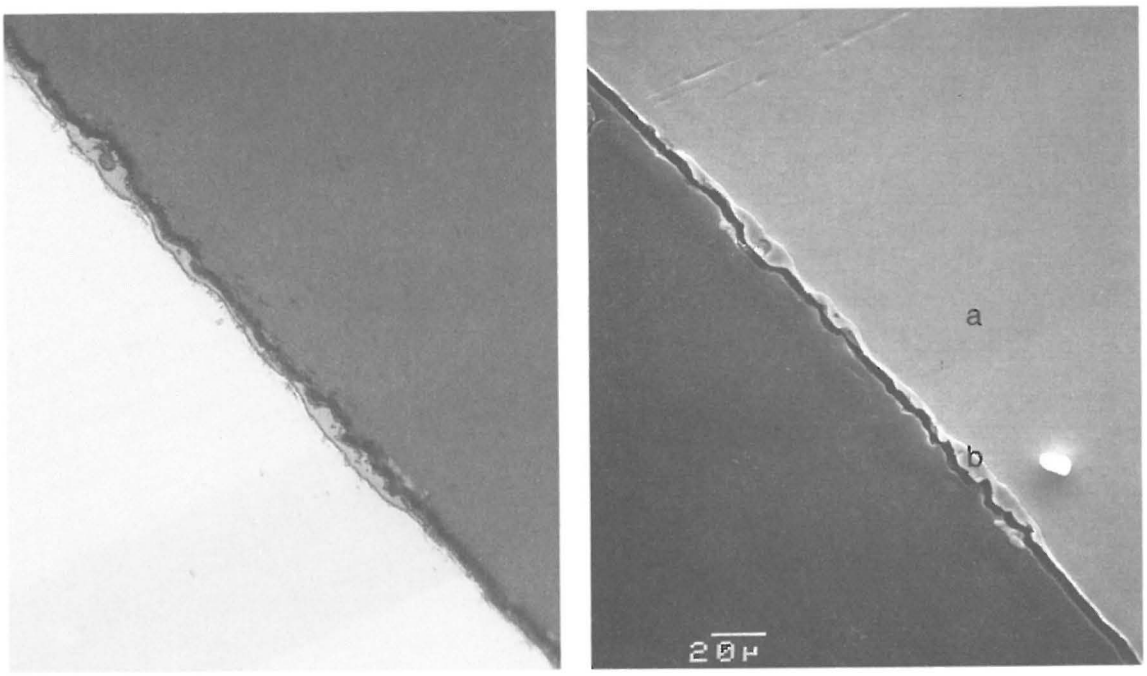

Fig. 20,21: Metallographic image (left) and mirror-inverted SEM image (right) of a Zircaloy-4 hull cross-section from the inside.
a: Zircaloy-4, b: Zirconium oxide.

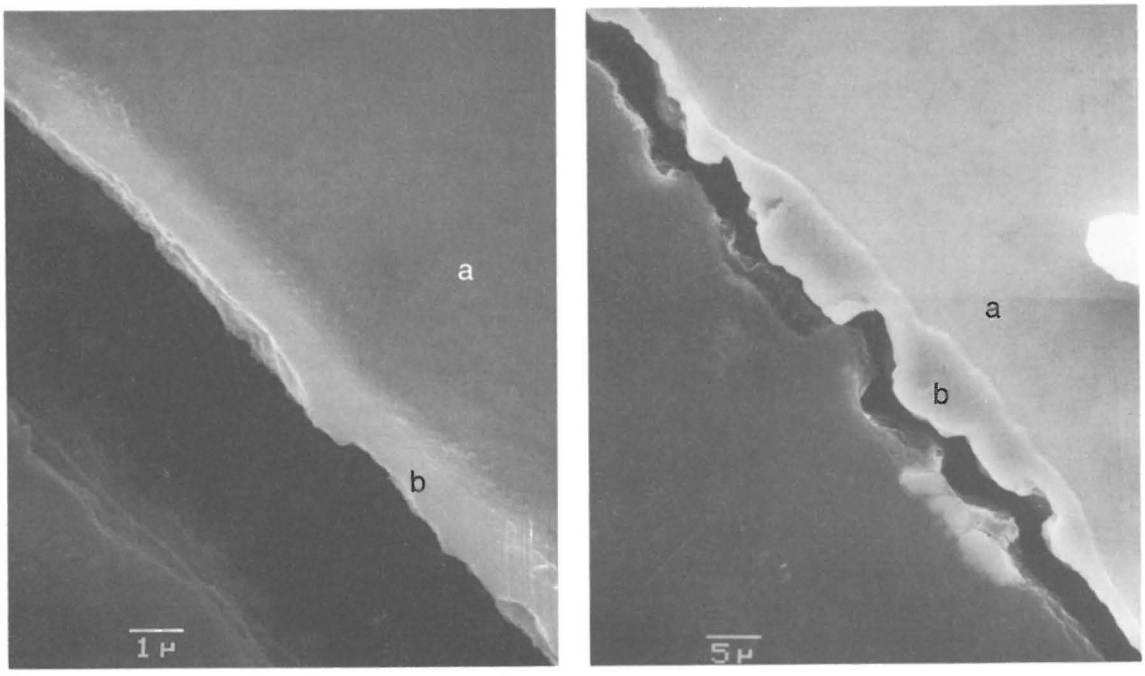

Fig. 22,23: SEM images of the Zircaloy inner surface. Extracts from Figure 21. Figure 22 (left) with normal oxide layer. Figure 23 with locally increased oxide layer.
a: Zircaloy-4, b: Zirconium oxide.

7.2 SEM analysis of the inner surface

Before the Zircaloy samples were examined under the scanning electron microscope (SEM), they were cut to a size of 8x8 mm, cleaned slightly and compressed for the SIMS analysis.

Following irradiation in the neutron field and hydride precipitation, it is to be expected that the material will become more brittle. The compressing process in particular then leads to the surface being permeated with parallel microcracks (Figures 24, 27, 28). Larger cracks were more likely caused by the "chopper" (Figure 25).

In addition to the predominantly smooth surface, there are also zones with a rough structure (Figures 24, 25, 27, 28). These zones look as if they have grown out of the ground material. At such locations, clear uranium signals were registered using EDS analysis. It can also be assumed that the other actinides are more easily trapped on such rough surfaces and that cleaning will be more difficult in such cases. These zones are particularly brittle and, given mechanical stressing, tend towards layerwise cracking (Figures 27, 28).

In the crack profile, the surface layer is granular down to a depth of 10-30 µm (Figure 26). This structure is therefore not restricted to the ZrO_2 layer, but continues far into the α-Zr(O) phase. Under this is the compact, solid base material.

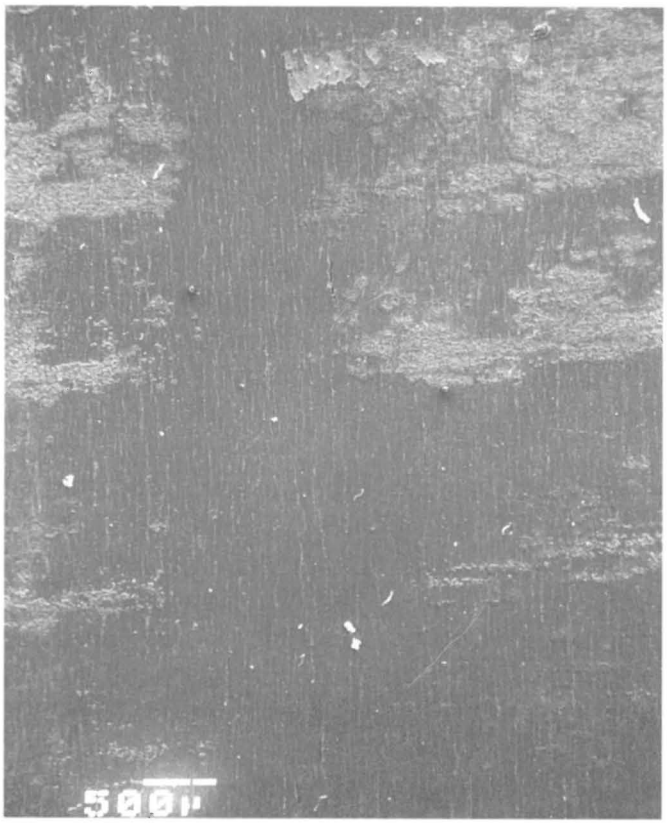

Fig. 24: SEM image of the Zircaloy hull inner surface. Rough zones in an otherwise relatively smooth environment.

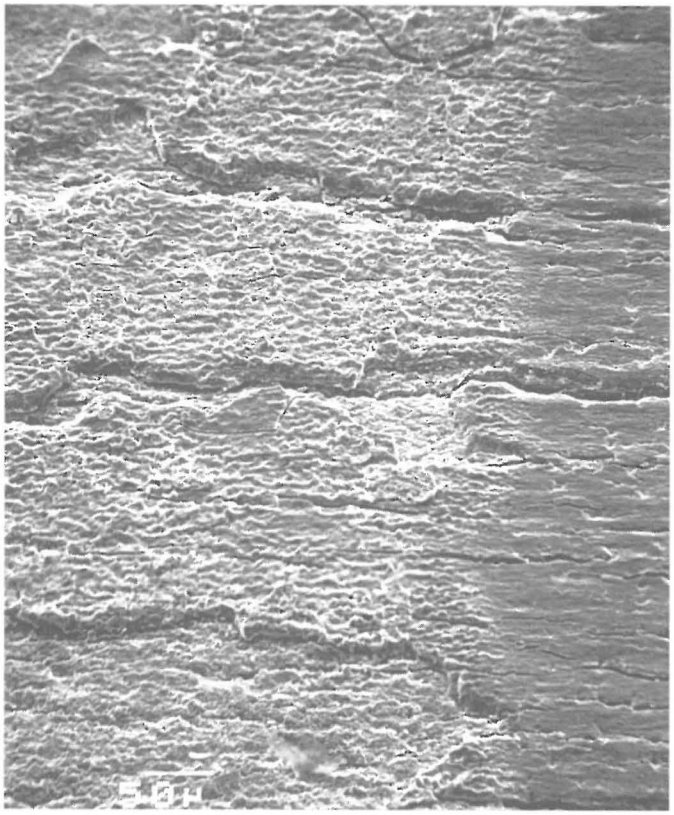

Fig. 25: SEM image. Left: fractured rough inner surface with partly exfoliated sheets. Right: undisturbed zone.

Fig. 26: Section from Figure 25. Profile of a fractured location with typical granulated surface.

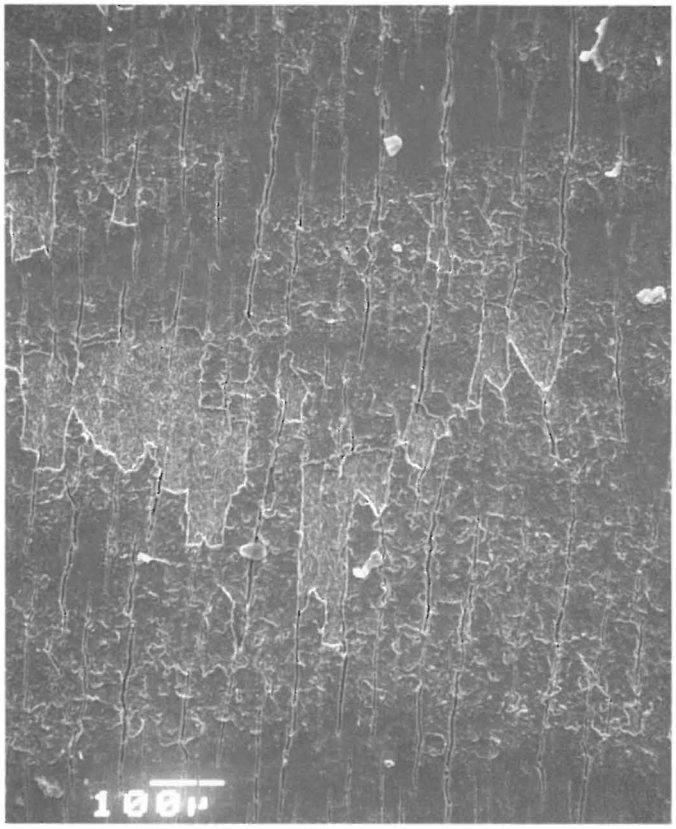

Fig. 27: Exfoliated inner surface layers.

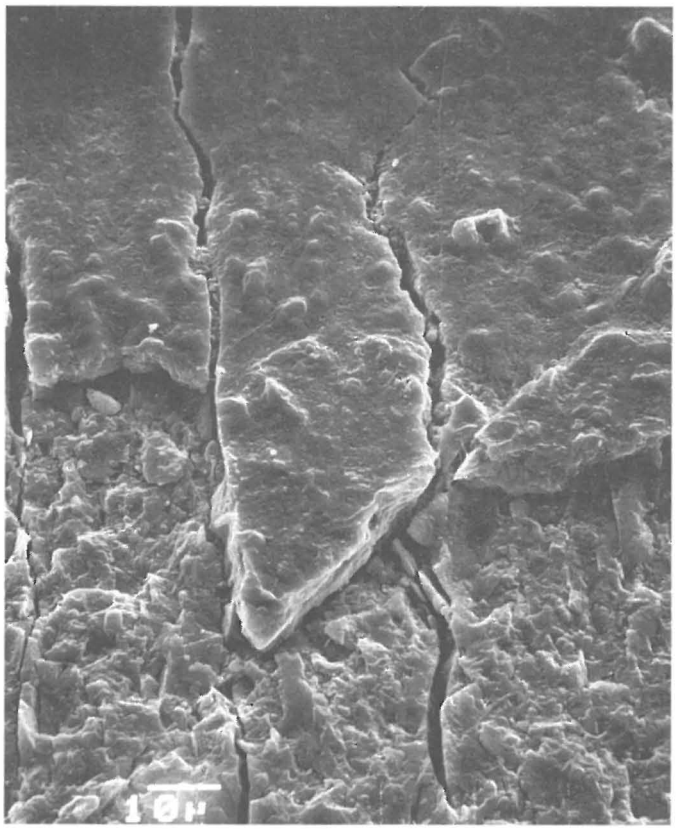

Fig. 28: Section from Figure 27.

8 CONCLUSIONS AND RECOMMENDATIONS

The cladding waste investigated in this work arises from the chop-leach process in industrial reprocessing and is made up of Zircaloy hulls from the fuel rods and around 25 wt-% of Inconel and stainless steel from the fuel element assembly. It should be noted that the fuel assembly end caps and the so called "fines" are not part of the cladding waste investigated in this work. These metallic residues are contaminated and it is a requirement that these be characterised as accurately as possible for disposal purposes. The results of such characterisations are also used for designing assay or other monitoring set-ups. Finally these results can also be used to improve the method used for rinsing of the hulls to reduce activity levels.

The investigations carried out on the PWR cladding material paid particular attention to the first aspect, namely measuring nuclide-specific activity concentrations and their local distribution. The most important analytical radiochemical data are summarised in Tables a and b of pages IV and V of the Summary.

The activation products within the fuel element structural materials (e.g. Co-60) make up the main source of the cladding activity (Table 1), these (beta gamma) activation nuclides result in a high gamma dose rate. In the case of the Zircaloy-4 hulls it is the fission products that dominate the activity with Sb-125 as the only notable activation product. However, the structural materials (stainless steel and Inconel) are also contaminated with fission products, although they only come into contact with the fuel in the dissolver. This indicates that deposits from the fuel solution represents a significant source of contamination. An attempt was made to calculate the beta,gamma activities for each specific material but, because of the large variation in the content of the activated elements (Co, Fe, Ni) in the structural components, it was only possible to give an overall estimate (Table 1).

Long-lived, highly toxic actinides are very important when assessing radiologically hazardous potentials and particular attention was therefore paid to characterising these nuclides. After a five-year cooling period, the mean alpha activity of the Zircaloy hulls is 6.7 mCi/kg Zry (250 MBq/kg Zry) and is made up mostly of the nuclides Pu-238, Pu-239, Pu-240, Am-241 and Cm-244. It is assumed that the alpha contamination of the structural materials is similar to, but not higher than, that of the hulls, since in the case of the former, only secondary contamination in the dissolver causes contamination. The large variation in the distribution of the actinide contents (380 to 2,130 mg U/kg Zry and 6 to 25 mg Pu/kg Zry) indicates the existence of certain heterogeneities. This was confirmed by optical and α-autoradiography investigations, when significant amounts of fuel residues were found in crushed or half-closed hulls.

SIMS analysis showed that uranium adheres mainly to the Zircaloy surface and that the concentration in the outer and inner oxide layer (in the first 2 μm) drops markedly. During irradiation, the fission products penetrate a considerable

distance into inner surface as recoil particles (Cs around 10 µm). This effect decreases significantly the local variation of the fission product activities as compared to the mentioned local variation of the actinide activities. On the outer hull surface the deposition behaviour of the fission products is similar to that shown by uranium.

The transuranic distribution is relatively even on the outer hull surface, while on the inside there are often locations with very high concentrations. This α-activity generally adheres fairly loosely and is likely to be reduced significantly using a suitable cleaning method. The nature and constancy of the U- and Pu-isotopic compositions, together with the surface analysis, imply that the α-contamination is more likely to have been caused by deposition from the fuel solution rather than by undissolved fuel. Besides these 2 mechanisms, there is a so called "low ground α-contamination", which will be more difficult to remove. This contamination is made up, on the one hand, of deposits of readily hydrolysable actinides and preferentially absorbed plutonium (in the tetravalent state). On the other hand, to a lesser extent, it is also made up of actinide penetration by thermal diffusion, recoil energy and corrosion processes.

To summarise, the parameters influencing the alpha contamination of the fuel rod hulls can be arranged in order of importance as follows:

- deposition from the fuel solution
- undissolved fuel (but also contamination in powder form arising from different measurement manipulation processes (GUÉ et al. 1987))
- absorption phenomena
- irradiation:
  fuel/cladding interaction (corrosion), migration via thermal diffusion and recoil energy, production of alpha emitters during the n-irradiation from cladding uranium and thorium impurities

The following factors promote the first three processes above:

- hull deformation due to the action of the bundle shears which traps fuel and fuel solution residues and makes leaching difficult
- rough and even partly fractured surfaces
- deficiencies in dissolution and, especially, rinsing processes (static dissolver, low acidity solution (GUÉ et al. 1987).

Due to the partial incorporation of fission products into the metallic surface, improving the rinsing process has less effect on their removal as compared to actinide contamination. The difference in leaching behaviour also explains the lack of correlation between Cs-137 and uranium. As a result, Cs-137 is not considered to be suitable as a key nuclide for scaling the remaining alpha contamination in control or assay procedures.

The analysis carried out largely confirm the CEA results (GUÉ et al. 1987). The results of the surface analysis allowed the postulated contamination mechanisms to be confirmed.

The hull and structural material debris investigated in this work are conditioned in cement and packaged in specific containers by the reprocessors (COGEMA, BNFL). This waste sort also includes the fuel element ends and part of the insoluble fines from the chop-leach process. Although it is estimated that these additional materials do not lead to a significantly higher α-inventory, analysis of these components are recommended.

Recommendations for further analyses are:

- investigation of the fuel rod material for MOX fuel. The U/Pu ratio in this case will be completely different and the level of alpha activity could increase considerably

- investigation of cladding waste from the new UP-3 plant at la Hague. The rotating dissolver of this plant may well reduce the loosely bound α-contamination

- investigation of high burn-up fuel assemblies (α-deposition in thicker oxide layers, pellet - cladding interaction)

Analyses of BWR cladding material are of lower priority since work to date indicates no significant differences from PWRs. In addition measurements of long-lived β-active nuclides are also of low priority (Tc-99, Pd-107, Cs-135, etc.) as calculations have shown the quantities of these radionuclides to be low (ORIGEN code, etc.).

9 ACKNOWLEDGEMENTS

J.C. Alder, Nagra, for initiating and managing this project and for establishing the necessary contacts to CEA.

J.P. Gué, CEA, for discussions and suggestions of an analytical nature.

C. Friedli, EPFL, for the Sr-90 analysis.

EDF/DER, Clamart, for radial Pu isotope calculations and Chr. Ott, PSI, for the evaluation.

Mr. Sommer and Mr. Riedel, KKW Obrigheim, for burn-up information.

Th. Bühler and D. Winkler for assisting with the isotope dilution analysis.

M. Mohos for the SEM recordings.

A. Erne for the metallography.

W. Görlich for the α spectrometry and D. Orciuolo for the mass spectrometry.

10 REFERENCES

DEGUELDRE, C.A. 1984: Neptunium neutron activation analysis. EIR-TM-42-84-24.

DILLON, R.L. 1976: Cladding Hulls, Proceedings of the international symposium on the management of wastes from LWR fuel cycle. Denver, Colorado.

GROSSMAN, L.N. & ROONEY, D.M. 1965: Interfacial reaction between UO2 and Zircaloy-2. General Electric report No. GEAP-4679, San José, CA.

GUÉ, J.P., ISAAC, M. & MIQUEL, P. 1982: Premières données sur la contamination des coques provenant du retraitement des combustibles des réacteurs à eau. Meeting on conditioning and storage of spent fuel element hulls. Brussels, January 1982.

GUÉ, J.P., ISAAC, M., MASSON, M., PHILIPPE, M., MALET, G., MOUCHNINO, M., ADAM, A., MANENT, G., BOSSER, R. & ROMEYER-DHERBEY, J. 1987: Détermination de la composition et de la radioactivité des coques provenant du traitement industriel des combustibles des réacteurs à eau légère. "Opération Coquenstock". Rapport final, CCE Bruxelles, EUR 10923 FR.

HEBEL, W. & COTTONE, G. 1982: Conditioning and storage of spent fuel element hulls. Radioactive waste management, volume 9, Proceedings, Brussels, January 1982. Harwood academic publishers for the CEC.

HOFMANN, P. & KERWIN-PECK, D. 1984: J. Nucl. Mat., 124, 80.

JENKINS, I.L., BOLUS, D.J., GLOVER, K.M., HAYNES, J.W., MAPPER, D., MARWICK, A.D. & WATERMAN, M.J. 1982: The characterisation of activities associated with irradiated fuel element claddings. Commission of the European Communities, Nuclear Science and Technology, Brussels, Report O: EUR 7671 EN.

MALLETT, M.W. et al. 1957: The Zirconium-Uranium dioxide reaction, Battelle Report No. BMI-1210, Columbus (Ohio).

REILLY, T.D. 1979: The measurement of leached hulls; informal report LASL LA-7784 MS, Los Alamos.

RESTANI, R., LINDER, H.P. & MÜLLER, A. 1986: Übersichtsanalysen an PWR-Brennstabhüllen aus der Wiederaufarbeitung. EIR-TM-42-86-18.

RESTANI, R. & MÜLLER, A. 1987: Alpha-Autoradiographie von Brennstabhüllen aus der Wiederaufarbeitung. EIR-TM-42-87-21.

VEHLOW, J. 1985: Werkstoffe und Korrosion, 36, 195.

WERTENBACH, H. 1984: Determination of nuclear fuel residues in dissolver sludge and on hulls after reprocessing. International conference on nuclear and radiochemistry, Lindau.

11 APPENDIX: Actinide analysis

11.1 Dissolution of Zircaloy hull fragments

The Zircaloy samples weighed 4-4.8 g. According to data from the CEA, they were dissolved in 3M HNO_3 and 2M HF, using the following procedure for the upper weight class.

1. Prepare 2.6 g $B(OH)_3$ (s)
2. Add 54 ml distilled water, shake well and, if necessary, warm till the $B(OH)_3$ has dissolved
3. Add 16.7 ml conc. HNO_3
4. Add 7.1 ml 40 % HF solution

For the dissolution the Zircaloy sample was placed together with 10 ml of water in a 500 ml teflon Erlenmeyer flask. The 80 ml solution was added dropwise with constant stirring in order to avoid too violent a reaction following dissolution of the oxide layer. The time required for dissolution was around 2 hours. The sediments were then filtered and dissolved with a solution of 0.41 g $B(OH)_3$, 5.4 ml 7M HNO_3 and 5.7 ml HF (1:1). It was sometimes necessary to heat the suspension to 70° C to ensure complete dissolution.

The whole solution was made up to 100 g and formed the original solution A for subsequent analysis.

11.2 Isotope dilution analysis of uranium and plutonium

ASTM standard methods[1] were followed for the analysis.

11.2.1 Preparation

Of the 100 g of original solution A, two 4 g (approx.) aliquots B are transferred each time to the laboratory for analysis. Such a 4 g Zircaloy solution contains around 0.18 g Zr, 0.2 mg U and 2.5 µg Pu. One of the two aliquots must be accurately weighed as it is intended for the spiked solution.

---

[1] Annual Books of ASTM-Standards: E321 (1979), E244 (1983), E267 (1983)

The spikes U-233 and Pu-242 are available as standard solutions[2] and are extracted with a syringe (in each case around 0.3 ml) and weighed on a micro-balance. The two spikes are placed in a small evaporating basin and one of the two 4 g B aliquots is added.

11.2.2 Evaporation of spiked and unspiked aliquots

Each of the two solutions generates a gamma dose rate of approx. 4 mR/h at 25 cm, which means that work has to be carried out behind lead shielding. Because of the volatility of Ru-106 in the form of RuO_4, evaporation has to be carried out using special apparatus. This consists of a large Witt flask which is capable of taking both of the B solutions. This is heated with two IR lamps. The off-gases are cleaned in a washing column. A packed column with glass Raschig rings is connected to three gas washing bottles. The first contains a solution of 8M HNO_3 and 0.1M H_3PO_3 with the reducing agent $NaNO_2$ (conversion to RuO_2). The second bottle contains a solution of $NaOH/NaNO_2$, and the third a small amount of $NaNO_2$ in water. At the end of the apparatus, a vacuum pump provides a constant throughput of air which is regulated via a Woolf bottle.

The spiked Zr solution should be thoroughly mixed before evaporation. The two B aliquots are then evaporated to a specific residual humidity ($\rightarrow$ white cake). Each is then combined with around 2-3 ml conc. HNO_3 and 100 µl 0.01 M $(NH_4)_2Fe(SO_4)_2.6H_2O$ and left for five minutes (reduction of Pu(VI) to Pu(III), Pu(IV)). There is then another evaporation to residual humidity to eliminate HF. One normally works with disposable capillary pipettes (micropipettes).

11.2.3 Pu-valence conversion

2 ml of conc. HNO_3 + 200 µl 0.2 M $NaNO_2$ in a slightly basic solution (50 µl of 5 % NaOH per 100 ml) is added to each of the evaporated solutions. This is left to react and then evaporated to residual humidity. After evaporation, the samples are absorbed in approx. 1.5 ml 8M HNO_3, mixed well and left to stand. If the samples are left to stand overnight, 200 µl of $NaNO_2$ solution should be added the next day. Pu(III) and Pu(VI) are converted to Pu(IV). The $NaNO_2$ solution used should be relatively fresh.

---

[2] Standard solutions prepared from dissolution of oxidic ORNL-Standards
U-233: $1{,}588 \times 10^{17}$ atoms/g solution
Pu-242: $3{,}4943 \times 10^{16}$ atoms Pu-242/g solution + $5{,}8609 \times 10^{14}$ atoms Pu-239/g solution

11.2.4 Separation on an anion-exchange column

A column is prepared for each of the spiked and unspiked solutions. Quartz wadding plug and 2.6 cm of DOWEX 1x4,200/400 mesh, suspended in water, are filled into a small Pasteur pipette (inner diameter around 5 mm). The Cl^- ions in the resin are exchanged for NO_3^- ions using around 2 ml 4M HNO_3 (checked with $AgNO_3$ in the eluate). The columns are then conditioned using 2 ml 8M HNO_3, which reduces the length of the column to around 2 cm. If the columns are left to stand, the upper end of the column should be covered with "parafilm" to prevent the resin drying out.

The prepared samples are transferred to the relevant marked column. The solutions transferred should be as clear as possible, without suspension. The cakes of the evaporated B solutions are rinsed twice with 1 ml 8M HNO_3 and also brought to the column. 1 ml of 8M HNO_3 is added once directly to the column to wash out the fission products. The U(VI) is eluted portionwise with 5 ml HNO_3 (1:5) and caught in the evaporating basin. The columns are rinsed and the plutonium cleaned with 12 ml HNO_3 (1:5). The waste solution can be checked for the absence of uranium using NaOH (formation of $Na_2U_2O_7$). The more stable Pu-nitrate complexes are eluted using 5 ml HNO_3 (1:30). All of the washed-out Pu is then checked with a further 100 µl HNO_3 (1:30) by dropping the effluent onto filter paper and measuring it after drying.

A total of four samples are produced and prepared for cleaning.

11.2.5 Cleaning of uranium

- The uranium eluate is completely evaporated
- A few drops of conc. HCl are added and evaporated. Repeat once
- Redissolve in 0.5 ml HCl (1:1)
- The anion-exchange column is prepared using 5 mm DOWEX 1x4,200/400 mesh. Chloride ions are not exchanged. An IR lamp is mounted horizontally 50 cm from the column and switched on. Best results are achieved with 50-60 °C
- Column is rinsed with 2.5 ml HCl (1:24) and then conditioned with 2.5 ml HCl (1:1)
- Dissolved U-sample is brought to the column
- Column washed with 3-4 ml HCl (1:1) (waste solution)
- Uranium eluted with 1.25 ml HCl (1:24)
- Evaporate and prepare for mass spectrometry. Possible fuming with conc. HNO_3 (2x0.5 ml) to remove any resin residues from the ion-exchanger

11.2.6 Cleaning of plutonium

- Redissolve evaporated Pu eluate in 1 ml conc. HNO_3
- Evaporation only to 3 to 5 drops to prevent any low-solubility oxides forming
- Prepare column with 5 mm of anion-exchange resin DOWEX-1. Mount IR lamp and switch on
- Wash column with 2.5 ml HCl (1:24) then condition with 2.5 ml HNO_3 (1:1)
- Add around 5 drops of HNO_3 (1:1) to the Pu sample and transfer to the column. Rinse the evaporating basin with 5 drops of HNO_3 (1:1) and add to the column
- Wash column with 6 ml HNO_3 (1:5) (waste solution)
- Elute plutonium with 1.25 ml HCl (1:24)
- Evaporate and (possibly) fume with conc. HNO_3 (2x). Prepare for MS

11.2.7 Preparing filaments for mass spectrometry

a) Uranium

The cleaned, evaporated uranium is dissolved in 0.5 ml H_2O b.d., picked up with yellow pipette tips and transferred to plastic tubes.

A small indentation is made in the middle of the rhenium band using a micropipette and around 6 µl of solution is placed in this. Evaporation at 1.9 A current. Short (2 to 3 secs.) ignition at 4.5 A. Double samples should always be produced.

b) Plutonium

Dissolve the evaporated Pu in the evaporating basin with 200 µl 0.075 M HNO_3 and, as in the case of uranium, transfer onto the filament. Before making the filament red-hot at higher current, a minimum of 30 cts/s alpha should be measured on the rhenium band.

When loading, care should be taken to avoid any contamination, particularly when several samples are being loaded. Gloves should be checked for α-contamination, caps for sealing samples should be kept clean, pipette tips changed, etc.

11.2.8 Mass spectrometry

MS gives the isotopic composition in the case of the unspiked samples and, by measuring the isotope ratios Pu-242/Pu-239 or U-233/U-238, in the spiked samples, the respective quantities of isotopes.

11.3 α-spectrometry activity measurements of Zircaloy fission product solutions containing actinides

11.3.1 Introduction

The accuracy of the α-spectrometry measurements and the degree of resolution of the spectra are very dependent on the quality of sample preparation. The first experiments were therefore carried out using electro-chemical deposition from aqueous solutions. This procedure was based on the method developed by L. Hallstadius[3], combined with the critical rinsing and conditioning stage at the end of electrolysis developed by N.A. Talvitie[4]. However, Am and Cm could only be separated electrolytically with high yield and without cathode corrosion from Zircaloy-free solutions. Because of restricted time available, there was no attempt at selective separation of the zirconium and the fission products, and recourse was made to the established evaporation method[5]. However, for our analyses, this technique only had an accuracy of around ± 10 %. The methods discussed in the following paragraphs coincide largely with those in (GUÉ et al. 1987).

11.3.2 Manufacturing α-preparates for α-spectrometry

Stainless steel platelets (ϕ 28 mm) are used as carrier material. These are polished up to 1/4 µm diamond finish, cleaned and degreased (acetone). The surface is heated briefly (slightly golden) and thus rendered hydrophilic. The steel platelets are mounted on a rotating shaft. 100 µl of the solution to be analysed are transferred carefully to the circular surface of 2 cm^2.

To improve spreading of the solution, 10 µl TEG (tetraethyleneglycol) are added. The disc is then rotated slowly so that the solutions are thoroughly mixed. When the disc is rotating, the IR lamp is switched on and evaporation occurs slowly. The temperature should be gradually increased. Following evaporation, the platelet with the deposited activity is ignited for one minute in an oven at 600-800 °C.

---

(3) L. Hallastadius, Nuclear Instr. Meth. Phys. Res., 223 (1984) 266-67

(4) N.A. Talvitie, Anal. Chem., 44 (1972) 280

(5) R. Hurst, K.M. Glover, AERE C/M 100 (1951)

11.3.3 Measurement of total alpha activity

Around 0.5 g of the 100 g original A solution are removed and weighed. This aliquot is diluted with 2M HNO_3 to 25 ml (solution C). 100 µl of this solution, with an alpha activity of around 300-900 pCi, are evaporated on a s.s. disc using the above procedure for subsequent α-spectrometry[6]. Figure A-1 shows a typical spectrum.

11.3.4 Americium and curium analysis

3 ml (with approx. 4 nCi Am-241, 3 nCi Cm-244, 40 ng Pu) of the 25 ml C solution are evaporated in the glass apparatus with off-gas washing (cf. 11.2.2) to around 0.5 ml. RuO_4 and HF volatilise. 400 µl of conc. HNO_3 are then added and evaporated. The procedure is repeated once again, which should ensure a certain residual humidity (avoiding low-solubility plutonium oxides). The sample is then redissolved in 500 µl 8M HNO_3 and mixed with 50 µl 0.001M $(NH_4)_2Fe(SO_4)_2$. This is allowed to react for 5 minutes and hexavalent Pu is reduced. 25 µl of fresh, slightly basic 0.2M $NaNO_2$ solution is then added (cf. 11.2.3), allowed to react briefly then evaporated down to a few drops.

There is a choice of two solutions for extraction of tetravalent plutonium:

a) 10 Vol-% trioctylamine (TOA) in Xylene extracted with 4M HNO_3.
b) 0.5M thenoyltrifluoroacetone (TTA) in Xylene.

The evaporated sample is collected portionwise with 5 ml 4M HNO_3 and then extracted three times with 5 ml extraction solutions in a test glass tube. The aqueous phase with Am(III) and Cm(III) is removed by pipette and evaporated in a teflon beaker. This is fumed twice with conc. HNO_3 to remove organic residues then absorbed portionwise with approx. 3 ml 4M HNO_3 and filled into polyethylene vials. The samples are weighed accurately. Around 100 µl are required for the α-preparate (weight should be noted), which corresponds to an Am, Cm activity of 50-200 pCi each. The yield determination and calibration of the α measuring location is done using simulated standard solutions with Zircaloy, americium, curium and plutonium. Figure A-2 shows a typical α-spectrum after Pu separation.

---

[6] α-spectrometry with silicon surface barrier detector
- effective surface: 490 mm^2
- resolution: 50 keV
- working distance: 5 mm; vacuum in analyser cell ~ 2Pa
- calibration sources produced from Standard solutions

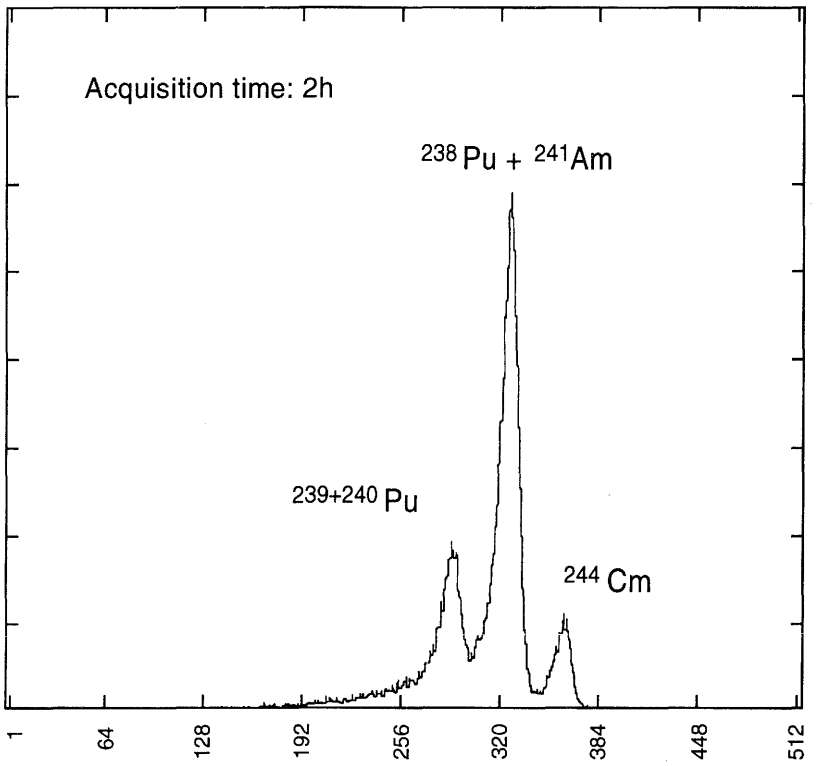

Fig. A-1: α-spectrum of a contaminated, dissolved Zircaloy hull sample 8 years after end of irradiation. α-activity of diluted sample: 955 pCi.

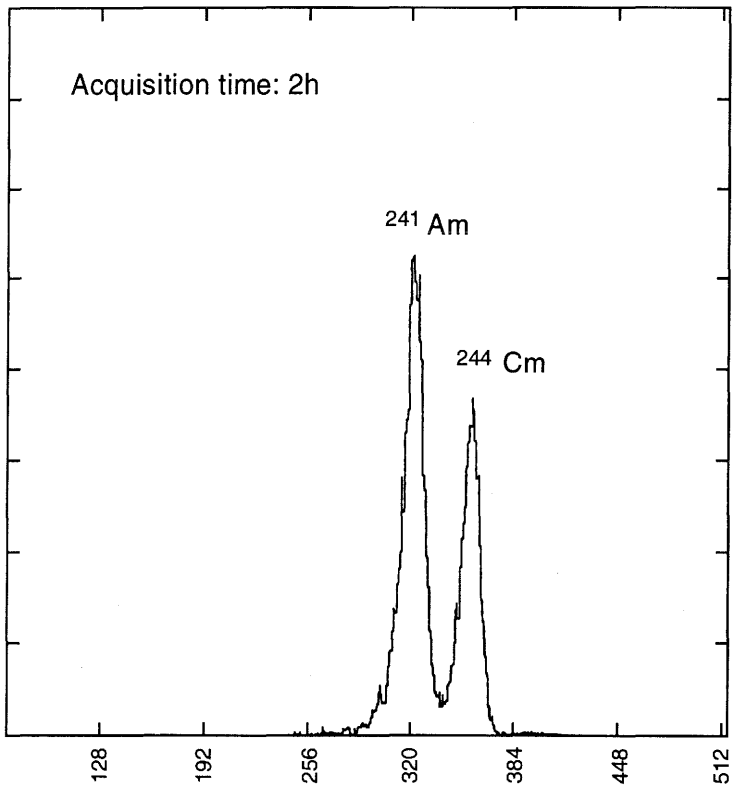

Fig. A-2: α-spectrum after Pu separation. 124 pCi Am-241, 97 pCi Cm-244.

11.4 Neptunium analysis

The very small quantities of long-lived Np-237 can be measured using neutron activation analysis (DEGUELDRE 1984). In order to eliminate disturbances of the gamma spectrometry of the generated Np-238 (984 keV gamma-line), the neptunium is isolated in several steps.

11.4.1 Preparing an oxidation cocktail

Around 8 g of the Zircaloy A solution are required for the analysis. Because of the high radiation levels (around 400 mR/h (gamma) at the flask surface), work has to be performed behind lead shielding with thick gloves.

Zirconium is complexed to ZrF_6^{2-} using NH_4F to allow it to be separated easily at a later stage. The excess of fluoride ions is bonded using Al^{3+} in order to prevent formation of low-solubility UF_4 and AmF_3. U, Pu and Np are brought to the hexavalent oxidation state using $K_2Cr_2O_7$. NH_4NO_3 is used as a salting-out agent for subsequent extraction of these three actinides.

The following substances should be mixed in the separating flask:

8 g Zircaloy solution (HF/HNO_3) contains approx. 0.4 g Zr, 0.5 mg U, 5 µg Pu, 150 ng Np

+ 1.9 ml 5M NH_4F
+ 88 mg $K_2Cr_2O_7$

Dissolve and allow to stand for around 15 minutes

+ 2.4 g $Al(NO_3)_3.9H_2O$
+ 13.5 g NH_4NO_3

This should be dissolved, stirred occasionally and heated slightly with the IR lamp. All components are dissolved after 1 to 2 hours. The quantity of solution is now 15-20 ml.

11.4.2 Extraction of U, Pu and Np

After cooling to ambient temperature, 9 ml MIK (methylisobutylketone) should be added to the above solution and extracted for 3 minutes. The organic phase is separated to the second separating flask. Repeat extraction in the first flask with 9 ml MIK and also transfer this organic phase to second flask.

Am(III), Cm(III), Zr and the fission products remain in the aqueous solution.

11.4.3 Washing out the extraction solution

The organic solution in the second separating flask (18 ml) is extracted for 3 minutes using 9 ml of saturated NH_4NO_3 in approx. 0.1M $Al(NO_3)_3$ solution[7]. The flask is then left to stand for around 2 hours till the solution is clear. The MIK should be pipetted off into a third separating flask. The aqueous solution still contains fission product residues and Am and Cm.

11.4.4 Backextraction

The organic phase is extracted three times with 4.5 ml 0.1M HNO_3 in the third flask.

11.4.5 Evaporation

Before evaporation, the approx. 13 ml of nitric acid solution is around 3 molar. It should be almost completely evaporated in a teflon beaker.

11.4.6 Reduction of Np(VI) to NP(IV)

The evaporated sample is withdrawn portionwise with a total of approx. 5 ml 0.4M HNO_3 and filled into a test glass tube. A higher HNO_3 concentration carries the danger of compensation of the reducing conditions which are created by addition of

0.1 ml 0.2M $(NH_4)_2Fe(SO_4)_2$
+ approx. 50 µl 2.5M $NH_2OH.HCl$

This solution is heated at 70 °C for 20 minutes, then allowed to cool and shaken for 15-20 minutes.

11.4.7 Extraction of Np(IV)

5 ml of 0.5M TTA in Xylene is added to the above aqueous solution and is extracted for 15 minutes in the apparatus and 3 minutes by hand. After separation of the phases (emulsion), the aqueous phase, which contains ura-

---

[7] Start with 0.2M $Al(NO_3)_3$-solution. Addition of NH_4NO_3 until sediments remain (end concentration just 0.1M $Al(NO_3)_3$).

nium and plutonium, is removed by pipette. The organic phase is washed three times with

3 ml 1M HNO_3
+ 0.1 ml 0.2M $(NH_4)_2Fe(SO_4)_2$
+ 50 µl 2.5M $NH_2OH.HCl$

for 5 minutes. The washing solutions are checked for α.

11.4.8 Backwashing of neptunium

The TTA phase is stripped with 3 ml 8M HNO_3 by extraction for 15 minutes. Fe(II) is oxidised and forms a reddish complex.

The aqueous phase with Np is transferred to the teflon beaker. Stripping with 3 ml 8M HNO_3 is repeated.

11.4.9 Evaporation

The 6 ml Np solution is evaporated in the teflon beaker using an IR lamp. The temperature is initially maintained at 60-80 °C (NO_x evolution), and is later increased to 80 °C. The residue is dissolved several times in conc. HNO_3 and evaporated until the organic residues have been eliminated.

11.4.10 Evaporation in quartz glass ampoules

The solution in the teflon beaker is transferred using a 50 µl pipette to a narrow quartz ampoule (ID 4 mm). This is filled only to 1.5 to 2 cm and then evaporated with very slight air supply (beware of delay in boiling). The teflon beaker is rinsed several times with conc. HNO_3. The evaporation time is several days.

11.4.11 Neutron irradiation

The quartz ampoules are irradiated together with a separate Np-237 standard for 48 hours using thermal neutrons of $2.5 \times 10^{13} n/(cm^2 \cdot s)$.

The yield of the separation procedure from TTA extraction is around 100 %. The total yield is only 70 %, which means that uncertainties of $\pm$ 20 % must be expected in the analysis.